TABLE II – PATHOLOGIC SIGNIFICANCE OF PROMOTER HYPERMETHYLATION OF *E-CADHERIN* IN EBV-ASSOCIATED GASTRIC CARCINOMA, AND DIFFUSE AND INTESTINAL SUBTYPES OF EBV-NEGATIVE GASTRIC CARCINOMA

	Frequencies of promoter hypermethylation						
	Total	Depth of invasion[a]			Lymph node metastasis		
		Early	Advanced	*p*	Negative	Positive	*p*
EBVaGC	95% (21/22)	100% (7/7)	94% (14/15)	NS	93% (14/15)	100% (7/7)	NS
EBVnGC diffuse[b]	65% (26/40)	100% (6/6)	59% (20/34)	0.0743	70% (7/10)	63% (19/30)	NS
EBVnGC intestinal[c]	46% (19/41)	29% (2/7)	50% (17/34)	NS	14% (2/14)	63% (17/27)	0.0038

[a]Early/advanced, tumor invasion within submucosa/tumor invasion beyond muscularis propria.–[b]EBV-negative GC showing diffuse type of histology. –[c]EBV-negative GC showing intestinal type of histology.

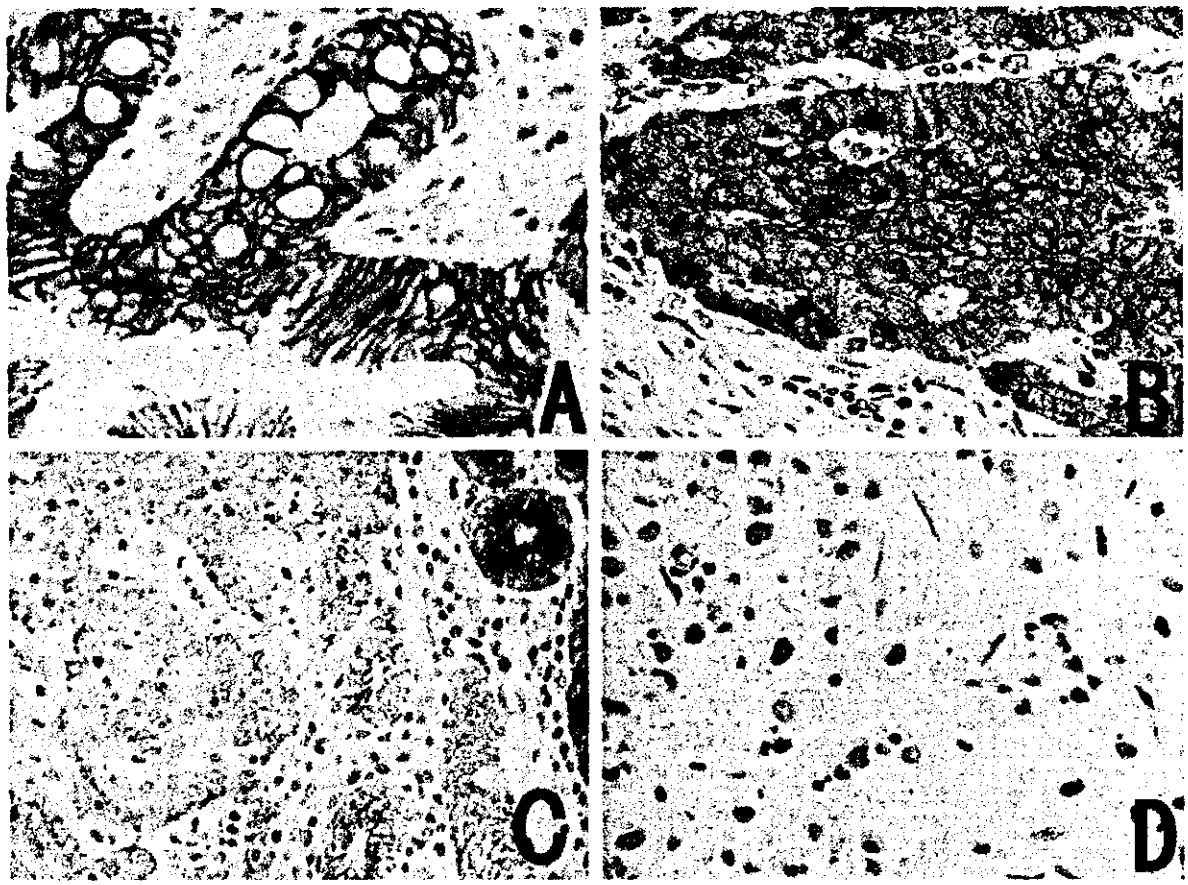

FIGURE 2 – Immunohistochemical staining pattern of E-cadherin in EBV-associated and EBV-negative gastric carcinoma. (*a*) Normal expression of E-cadherin in normal colonic mucosa. (*b*) Example of normal staining pattern in intestinal-type EBV-negative GC. (*c*) Heterogeneous staining pattern in EBVaGC. (*d*) Reduced staining pattern in diffuse-type EBV-negative GC. Original magnification × 400 for all panels.

amplification of microsatellite markers D16S265 and D16S301 was performed according to the procedures described by Machado *et al.*[19] PCR products were run in a 6% denaturing polyacrylamide gel with 5% crosslinking and exposed to X-ray film at room temperature overnight.

Regional heterogeneity of promoter hypermethylation of E-cadherin

Regional heterogeneity of promoter hypermethylation of *E-cadherin* was assessed in EBVaGC by the MSP analysis of the microdissected tumor tissue from the formalin-fixed, paraffin-embedded section. Two serial sections, 8 μm in thickness, were deparaffinized in xylene and rehydrated in alcohol. After the sections were briefly stained with hematoxyline, a 5 × 5 mm sized region was dissected from each with an 18 G needle tip. The tissue samples were treated with proteinase K (1 mg/ml) at 37°C overnight. After phenol-chloroform-isoamyl alcohol extraction and ethanol precipitation, each 1 μg of DNA was subjected to bisulfite modification as described above. Since the DNA was obtained from the formalin-fixed and paraffin-embedded sections, different primer sets were used to obtain shorter PCR products according the method of Herman *et al.*[25] The temperature profiles for the amplification were as follows: initial heating at 95°C for 5 min, 45 cycles of denaturation at 95°C for 45 sec, annealing at 57.0°C for

the methylated primer set and at 53.0°C for the unmethylated primer set and extension at 72°C for 45 sec, followed by a final extension at 72°C for 10 min.

Statistical analysis

Statistical analysis of the results was performed using the chi-square test or Fisher's exact test. Differences were considered to be significant at $p < 0.05$.

RESULTS

Promoter methylation of E-cadherin

Twenty-two cases of EBVaGC and 81 cases of EBV-negative GC were included in this study. The only significant difference between the 2 groups was the tumor location (cardia, gastric body in total cases: 22/22 in EBVaGC and 53/81 in EBV-negative GC).

The results of MSP analysis (Fig. 1) are presented in Table I. Nearly all of the carcinomas showed aberrant methylation of *E-cadherin* promoter in EBVaGC, and the frequency of this aberrant methylation was significantly higher in EBVaGC than in EBV-negative GC ($p = 0.0003$). The diffuse type of histology appeared to be correlated with the *E-cadherin* hypermethylation, albeit not to a statistically significant extent ($p = 0.0502$). Since 2/3 (15 of 22) of EBVaGC cases showed the diffuse type of histology, EBVaGC contributed to the relatively high frequency of aberrant methylation of *E-cadherin* in the diffuse type. Otherwise, the frequency of promoter hypermethylation did not differ significantly between any of the other groups classified by clinicopathologic factors such as age, gender, or location, depth of invasion and lymph node metastasis of the carcinoma.

Since E-cadherin is reported to relate to the histologic subtype of gastric carcinoma, EBV-negative GC was further divided into diffuse and intestinal types (Table II). The frequencies of aberrant methylation in these 2 subtypes of EBV-negative GC did not differ, and both were lower than the frequency in EBVaGC ($p = 0.0113$ and < 0.0001, respectively). However, the significance of the *E-cadherin* methylation appeared to be different in each subtype. When early and advanced stages were compared, the frequency of hypermethylation in the advanced stage (59%) was relatively lower than that in the early stage (100%) in the diffuse type of EBV-negative GC ($p = 0.0743$). On the other hand, the frequency of promoter hypermethylation increased as the tumor progressed from early (29%) to advanced carcinoma (50%) in the intestinal type of EBV-negative GC, albeit not to a statistically significant extent. The presence of lymph node metastasis was also found to be significantly correlated with promoter hypermethylation in this subtype of EBV-negative GC ($p = 0.0038$).

Immunohistochemistry of E-cadherin *and its correlation with promoter methylation*

Next, we investigated the expression of E-cadherin by immunohistochemistry in order to evaluate the correlation with promoter methylation. Both heterogeneous and reduced staining patterns were considered abnormal pattern (Fig. 2). Abnormal staining pattern was observed in 13 of 15 EBVaGC cases, 12 of 15 diffuse-type EBV-negative GC cases and 9 of 19 intestinal-type EBV-negative GC cases (Fig. 3). When the relationship between methylation status and immunohistochemical staining was analyzed in each subgroup, a significant correlation was noted only in the EBVaGC cases. On the other hand, significant number of the unmethylated cases showed abnormal staining pattern in the diffuse and intestinal types of EBV-negative GC cases.

Mutation and LOH of E-cadherin gene in EBVaGC

To exclude a possible contribution of genetic changes of *E-cadherin* in EBVaGC, PCR-SSCP was performed, and no mutation was observed in EBVaGC (Table III). MKN45 has 18 bp deletion at the exon 6-intron 6 boundary. At the experimental condition in the present study, the mutation of MKN45 was detected even when the percentage of MKN45 DNA was 10% in total DNA when mixed with DNA of nonneoplastic tissue. Similarly, LOH of *E-cadherin* was not observed in any of 11 cases examined (Table III).

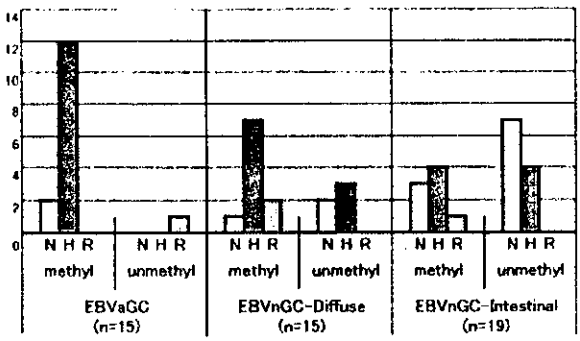

FIGURE 3 – Promoter methylation status and immunohistochemical staining patterns of E-cadherin in EBV-associated gastric carcinoma and diffuse and intestinal subtypes of EBV-negative gastric carcinoma. Twelve of 15 EBVaGC cases showed a heterogeneous staining pattern with promoter methylation, whereas this correlation was not observed in EBV-negative GC (EBVnGC). Methyl, methylated promoter; Unmethyl, unmethylated promoter; N, normal staining pattern; H, heterogeneous staining pattern; R, reduced staining pattern

Regional heterogeneity of promoter hypermethylation of E-cadherin in EBVaGC

To evaluate the regional heterogeneity of promoter hypermethylation of *E-cadherin* in EBVaGC, several samples were dissected from a section of each EBVaGC tumor (Table III). In 13 of 15 cases, the methylation status was successfully evaluated using the tissue samples of formalin-fixed and paraffin-embedded specimens (Table III). One of the cases evaluated did not show promoter methylation in the first evaluation using DNA derived from frozen tissue, but all of the cases showed methylation at least in one of the formalin-fixed samples. Heterogeneity of methylation status within the carcinoma was observed in all cases except 1 of 3 early carcinomas.

DISCUSSION

Epigenetic silencing of the gene expression by CpG island hypermethylation has been shown to play an important role in the carcinogenesis of various organs, including the stomach.[31–33] In recent investigations of EBVaGC cases, Kang *et al.*[9] and our own group[10] observed high frequencies of promoter methylation in various cancer-related genes such as *p14*, *p15*, *p16*, *DAPK*, *GSTP*, *TIMP-3* and *E-cadherin*, but not in *hMLH1* and *MGMT*. This finding suggests that a global but selective DNA hypermethylation of the cellular genes may occur in the EBV-infected epithelial cells. In the present study focusing on the E-cadherin protein of the stomach, we confirmed on a larger scale that nearly all of the carcinoma tissues of EBVaGC showed CpG island methylation of *E-cadherin*. Furthermore, we demonstrated that abnormal expression occurred in nearly all of EBVaGC cases, while such a correlation was not strictly observed in EBV-negative GC. Since neither mutation nor LOH was observed in EBVaGC, epigenetic silencing is a major mechanism of E-cadherin dysfunction in EBVaGC.

Most of the cases with hypermethylation in the present study showed a heterogeneous staining pattern rather than the reduced type in EBVaGC. This was consistent with our findings from earlier immunohistochemistry studies on p16 showing a marked decrease of p16 expression rather than a total loss of expression. Current studies on gene regulation by promoter methylation fit well with these findings. In cell lines from the human bladder, colon cancers and melanoma, Bender *et al.*[34] found that the ex-

TABLE III – EVALUATION OF MUTATION, LOH AND REGIONAL HETEROGENEITY OF PROMOTER HYPERMETHYLATION OF *E-CADHERIN* IN EBV-ASSOCIATED GASTRIC CARCINOMAS

	Case	Age	Gender	Histology	Depth[a]	Mutation[b]	LOH[c]	Methylation in frozen section[d]	Methyl[e]/sample[f]
1	J84	43	M	Diffuse	Early	–	–	+	1/3
2	F239	65	M	Diffuse	Early	–	–	+	1/2
3	J49	45	M	Intestinal	Early	–	–	+	3/3
4	F190	73	F	Diffuse	Advanced	ND	ND	+	1/4
5	F187	67	M	Diffuse	Advanced	ND	ND	+	2/5
6	F159	66	F	Diffuse	Advanced	–	–	+	1/5
7	F108	80	M	Diffuse	Advanced	–	–	+	1/3
8	F284	50	M	Diffuse	Advanced	–	–	+	1/3
9	F72	65	M	Diffuse	Advanced	–	–	+	2/4
10	F169	54	M	Diffuse	Advanced	ND	ND	–	1/3
11	J1	22	F	Intestinal	Advanced	–	–	+	1/4
12	F197	73	F	Intestinal	Advanced	ND	ND	+	1/3
13	J183	60	M	Intestinal	Advanced	–	–	+	3/5
14	F287	75	M	Intestinal	Advanced	–	–	+	Failed[g]
15	J150	62	M	Intestinal	Advanced	–	–	+	Failed[g]
16	J243	37	M	Intestinal	Early	ND	ND	+	ND
17	F196	65	M	Diffuse	Advanced	ND	ND	+	ND
18	F273	69	M	Diffuse	Advanced	ND	ND	+	ND
19	F63	34	M	Diffuse	Advanced	ND	ND	+	ND
20	F85	61	M	Diffuse	Advanced	ND	ND	+	ND
21	J355	62	M	Diffuse	Advanced	ND	ND	+	ND
22	J360	83	F	Diffuse	Advanced	ND	ND	+	ND

[a]Early/advanced, tumor invasion within submucosa/tumor invasion beyond muscularis propria.–[b]Result of mutation analysis by PCR-SSCP; –; no mutation was detected; ND, not done. –[c]–, no LOH was detected.–[d]+, methylated; –, unmethylated. –[e]Number of samples that showed promoter hypermethylation.–[f]Number of samples obtained from one tumor by microdissection. –[g]MSP was not successful.

pression of p16 is highly affected by the frequency of methylation of the *p16* promoter, but not by the presence of the methylation itself. Our study of the microdissection confirmed heterogeneity in the methylation status within each tumor. There are 2 explanations for this heterogeneity: hypermethylation occurs in a subpopulation of the carcinoma. Alternatively, the maintenance of hypermethylation is considerably disturbed in the progression of the carcinoma,[35,36] even though hypermethylation occurs in a uniform manner at early stage of cancer development. Methylation was observed in nearly all of the cases of EBVaGC, and the case showing methylation in all of the samples was the early gastric carcinoma in the present study. Thus, the latter possibility would constitute the most likely mechanism in EBVaGC.

As for the discrepancy between promoter methylation and gene expression in EBV-negative GC, regional heterogeneity of promoter methylation might exert in the cases of positive methylation but normal expression. On the other hand, in the cases of negative methylation but abnormal expression, at least 3 mechanisms[37] are possible: gene mutation,[18,30] posttranslational truncation or modification[38] and transcriptional repressor.[38–41] Thus, other than EBVaGC, further studies are necessary to disclose the regulation of *E-cadherin* gene expression in GC.

As an additional result, the present study provides some detailed statistical insights into the correlation between promoter methylation, gene expression/localization, tumor stages and tumor type in EBV-negative GC. In the intestinal-type EBV-negative GC, promoter hypermethylation of *E-cadherin* was correlated with both lymph node metastasis and invasion beyond the muscular layer. Since promoter methylation was not faithfully reflected in overall gene expression, promoter-methylated subpopulation within the tumor may play a primary role in the progression of this type of gastric carcinoma. On the other hand, the frequency of hypermethylation decreased from 100% to 59% as the carcinomas progressed from early to advanced in diffuse type. The maintenance of hypermethylation may be considerably disturbed in the progression of the carcinoma of the diffuse type of EBV-negative GC, as in the case of EBVaGC.

In conclusion, in addition to p16, the abnormality of E-cadherin expression caused by the aberrant methylation of *E-cadherin* gene promoter is closely associated with the development of EBVaGC. As the significance of aberrant methylation of *E-cadherin* differs between EBVaGC and EBV-negative GC, we can conclude that the recognition of this type of gastric carcinoma is critical for the evaluation of carcinogenesis of the stomach.

REFERENCES

1. Fukayama M, Chong JM, Kaizaki Y. Epstein-Barr virus and gastric carcinoma. Gastric Cancer 1998;1:104–14.
2. Fukayama M, Chong JM, Uozaki H. Pathology and molecular pathology of Epstein-Barr virus-associated gastric carcinoma. In: Takada K, editor. Epstein-Barr virus and human cancer. Berlin: Springer-Verlag, 2001. 91–102.
3. Fukayama M, Hayashi Y, Iwasaki Y, Chong JM, Ooba T, Takizawa T, Koike M, Mizutani S, Miyaki M, Hirai K. Epstein-Barr virus-associated gastric carcinoma and Epstein-Barr virus infection of the stomach. Lab Invest 1994;7:73–81.
4. Chong JM, Sakuma K, Sudo M, Osawa T, Ohara E, Uozaki H, Shibahara J, Kuroiwa K, Tominaga S, Hippo Y, Aburatani H, Funata N, et al. Interleukin1β expression in human gastric carcinoma with Epstein-Barr virus infection. J Virol 2002;76:6825–31.
5. Chong JM, Fukayama M, Hayashi Y, Funata N, Takizawa T, Koike M, Muraoka M, Kikuchi-Yanoshita M, Mizuno S. Expression of CD44 variants in gastric carcinoma with or without Epstein-Barr virus. Int J cancer 1997;74:450–4.
6. Sugiura M, Imai S, Tokunaga M, Koizumi S, Uchizawa M, Okamoto K, Osato T. Transcriptional analysis of the Epstein-Barr virus gene expression in EBV-positive gastric carcinoma: unique viral latency in the tumor cells. Br J Cancer 1996;74:625–31.
7. zur Hausen A, Brink AATP, Craanen ME, Middeldrop JM, Meijer CJLM, van den Brule AJC. Unique transcription pattern of Epstein-Barr virus (EBV) in EBV-carrying gastric adenocarcinomas: expression of the transforming BARF1 gene. Cancer Res 2000;60:2745–8.
8. Chong JM, Fukayama M, Hayashi Y, Takizawa T, Koike M, Konishi M, Kikuchi-Yanoshita R, Miyaki M. Microsatellite instability in the progression of gastric carcinoma. Cancer Res 1994;54:4595–7.
9. Kang GH, Lee S, Kim WH, Lee HW, Kim JC, Rhyu MG, Ro JY. Epstein-Barr virus-positive gastric carcinoma demonstrates frequent aberrant methylation of multiple genes and constitutes CpG island methylator phenotype-positive gastric carcinoma. Am J Pathol 2002; 160:787–94.
10. Chong JM, Sakuma K, Sudo M, Ushiku T, Uozaki H, Shibahara J, Nagai H, Funata N, Taniguchi H, Aburatani H, Fukayama M. Global

and non-random CpG-island methylation in gastric carcinoma associated with Epstein-Barr virus. Cancer Sci 2003;94:76–80.
11. Osawa T, Chong JM, Sudo M, Sakuma K, Uozaki H, Shibahara J, Nagai H, Funata N, Fukayama M. Reduced expression and promoter methylation of *p16* gene in Epstein-Barr virus-associated gastric carcinoma. Jpn J Cancer Res 2002;93:1195–200.
12. Takeichi M. Morphogenetic roles of classic cadherins. Cur Opin Cell Biol 1995;7:619–27.
13. Takeichi M. Cadherin cell adhesion receptors as morphogenetic regulator. Science 1991;251:1451–5.
14. Bracke ME, van Roy FM, Mareel MM. The E-cadherin/catenin complex in invasion and metastasis. In: Gunther U, Birchmeier W, eds. Attempts to understand metastasis formation. Berlin: Springer-Verlag, 1996. 123–61.
15. Shino Y, Watanabe A, Yamada Y, Tanase M, Yamada T, Matsuda M, Yamashita J, Tatsumi M, Miwa T, Nakano H. Clinicopathologic evaluation of immunohistochemical E-cadherin expression in human gastric carcinomas. Cancer 1995;76:2193–201.
16. Shun CT, Wu MS, Lin JT, Wang HP, Houng RL, Lee WJ, Wang TH, Chuang SM. An immunohistochemical study of E-cadherin expression with correlations to clinicopathological features in gastric cancer. Hepato-Gastroenterology 1998;45:944–9.
17. Oka H, Shiozaki H, Kobayashi K, Tahara H, Tamura S, Miyata M, Doki Y, Iihara K, Matsuyoshi N, Hirano S, Takeichi M, Mori T. Immunohistochemical evaluation of E-cadherin adhesion molecule expression in human gastric cancer. Virchows Arch 1992;421:149–56.
18. Becker KF, Atkinson NJ, Reich U, Becker I, Nekarda H, Siewert JR, Hofler H. *E-cadherin* gene mutations provide clues to diffuse type gastric carcinomas. Cancer Res 1994;54:3845–52.
19. Machado JC, Soares P, Carneiro F, Rocha A, Beck S, Blin N, Berx G, Sobrinho-Simoes M. *E-cadherin* gene mutations provide a genetic basis of the phenotypic divergence of mixed gastric carcinomas. Lab Invest 1999;79:459–65.
20. Tamura G, Sakata K, Nishizuka S, Maesawa C, Suzuki Y, Iwaya T, Terashima M, Saito K, Satodate R. Inactivation of the *E-cadherin* gene in primary gastric carcinomas and gastric carcinoma cell lines. Jpn J Cancer Res 1996;87:1153–9.
21. Guilford P, Hopkins J, Harraway J, McLeod M, McLeod N, Harawira P, Taite H, Scoular R, Miller A, Reeve AE. E-cadherin germline mutations in familial gastric cancer. Nature 1998;392:402–5.
22. Wu MS, Shun CT, Wu CC, Hsu TY, Lin MT, Chang MC, Wang HP, Lin JT. Epstein-Barr virus-associated gastric carcinomas: relation to *H. pylori* infection and genetic alterations. Gastroenterology 2000; 118:1031–8.
23. Japanese Gastric Cancer Association. Japanese classification of gastric carcinoma: 2nd English edition. Gastric Cancer 1998;1:10–24.
24. Lauren P. The two histological main types of gastric carcinoma, diffuse and so-called intestinal-type carcinoma. Acta Pathol Microbiol Scand 1965;64:31–49.
25. Herman JG, Graff JR, Myohanen S, Nelkin BD, Baylin SB. Methylation-specific PCR: a novel PCR assay for methylation status of CpGislands. Proc Natl Acad Sci 1996;93:9821–6.
26. Kallakury BVS, Sheehan CE, Winn-Deen E, Oliver J, Fisher HAG, Kaufman RP, Ross JS. Decreased expression of catenins (α and β), p120 CTN, and E-cadherin cell adhesion proteins and *E-cadherin* gene promoter methylation in prostatic adenocarcinomas. Cancer 2001;92:2786–95.
27. Shimoyama Y, Hirohashi S. Expression of E- and P-cadherin in gastric carcinomas. Cancer Res 1991;51:2185–92.
28. Jawhari A, Jordan S, Poole S, Browne P, Pignatelli M, Farthing MJG. Abnormal immunoreactivity of the E-cadherin-catenin complex in gastric carcinoma: relationship with patient survival. Gastroenterology 1997;112:46–54.
29. Berx G, Becker KF, Hofler H, van Roy F. Mutations of the human E-cadherin (CDH1) gene. Hum Mutat 1998;12:226–37.
30. Oda T, Kanai Y, Oyama T, Yoshiura K, Shimoyama Y, Birchmeier W, Sugimura T, Hirohashi S. *E-cadherin* gene mutations in human gastric carcinoma cell lines. Proc Natl Acad Sci 1994;91:1858–62.
31. Tamura G, Yin J, Wang S, Fleisher AS, Zou TT, Abraham JM, Kong DH, Smolinski KN, Wilson KT, James SP, Silverberg SG, Nishizuka S, et al. *E-cadherin* gene promoter hypermethylation in gastric carcinomas. J Natl Cancer I 2000;92:569–73.
32. Machado JC, Oliveira C, Carvalho R, Soares P, Berx G, Caldas C, Seruca R, Carneiro F, Sobrinho-Simoes M. *E-cadherin* gene (CDH1) promoter methylation as the second hit in sporadic diffuse gastric carcinoma. Oncogene 2001;20:1525–8.
33. Oue N, Motoshita J, Yokozaki H, Hayashi K, Tahara E, Taniyama K, Matsusaki K, Yasui W. Distinct promoter hypermethylation of p16(INK4a), CDH1, and RAR-beta in intestinal, diffuse-adherent, and diffuse-scattered type gastric carcinomas. J Pathol 2002;198:55–9.
34. Bender CM, Pao MM, Jones PA. Inhibition of DNA methylation by 5-aza-2'-deoxycytidine suppresses the growth of human tumor cell lines. Cancer Res 1998;58:95–101.
35. Joo YE, Rew JS, Kim HS, Choi SK, Park CS, Kim SJ. Changes in the E-cadherin-catenin complex expression in early and advanced gastric cancers. Digestion 2001;64:111–9.
36. Graff JR, Gabrielson E, Fujii H, Baylin SB, Herman JG. Methylation patterns of the E-cadherin 5' CpG island are unstable and reflect the dynamic, heterogenous loss of E-cadherin expression during metastatic progression. J Biol Chem 2000;275:2727–32.
37. Rosivatz E, Becker I, Specht K, Fricke E, Luber B, Busch R, Hofler H, Becker KF. Differential expression of the epithelial-mesenchymal transition regulators Snail, SIP1, and Twist in gastric cancer. Am J Pathol 2002;161:1881–91.
38. Rashid MG, Sanda MG, Vallorosi CJ, Rios-Doria J, Rubin MA, Day ML. Posttranslational truncation and inactivation of human E-cadherin distinguishes prostate cancer from matched normal prostate. Cancer Res 2001;61:489–92.
39. Cano A, Perez-Moreno MA, Rodrigo I, Locascio A, Blanco MJ, del Barrio MG, Portillo F, Nieto MA. The transcription factor Snail controls epithelial-mesenchymal transitions by repressing E-cadherin expression. Nat Cell Biol 2000;2:76–83.
40. Batlle E, Sancho E, Franci C, Dominguez D, Monfar M, Baulida J, de Herreros AG. The transcription factor Snail is a repressor of *E-cadherin* gene expression in epithelial tumour cells. Nat Cell Biol 2000;2:84–9.
41. Comijn J, Berx G, Vermassen P, Verschueren K, van Grunsven L, Bruyneel E, Mareel M, Huylebroeck D, van Roy F. The two-handed E box binding zinc finger protein SIP1 down regulates E-cadherin and induces invasion. Mol Cell 2001;7:1267–78.

Mol. Cells, Vol. 16, No. 2, pp. 143-146

Molecules and Cells

Nicotine Enhances Neovascularization and Promotes Tumor Growth

Takeshi Natori, Masataka Sata[1,2], Miwa Washida[1], Yasunobu Hirata[1], Ryozo Nagai[1], and Masatoshi Makuuchi*

Department of Surgery, University of Tokyo, Graduate School of Medicine, Tokyo 113-8655, Japan;
[1] Department of Cardiovascular Medicine, University of Tokyo, Graduate School of Medicine, Tokyo 113-8655, Japan;
[2] PRESTO, Japan Science and Technology Agency, Saitama 332-0012, Japan.

(Received December 11, 2002; Accepted May 21, 2003)

Solid tumors require vascularization for their growth. Bone marrow-derived endothelial progenitor cells participate in tumor angiogenesis. Here, we show that nicotine markedly accelerated growth of colon cancer cells inoculated subcutaneously in mice but had no effect on proliferation of carcinoma cells *in vitro*. We found that the tumor growth was associated with increased vascularization of the tumor and that bone marrow-derived cells contributed to the formation of the new blood vessels. Our findings show that nicotine promotes tumor growth, at least in part, by stimulating tumor-associated neovascularization.

Introduction

Cigarette smoking is the most important risk factor for cardiovascular disease and cancer, both of which are major causes of death in Western countries (Bartecchi *et al.*, 1994). In particular, 85% of lung cancers are attributable to smoking. Smoking also increases the risk of cancers of other organs, including mouth, pharynx, larynx, esophagus, stomach, pancreas, uterine cervix, kidney, ureter and bladder. However, the mechanism by which smoking increases cancer morbidity remains unknown.

Solid tumors require neovascularization for their growth (Folkman; 1990; 1995; Heeschen *et al.*, 2001; Lyden *et al.*, 2001; O'Reilly *et al.*, 1994). Here we show that nicotine, a major component of cigarette smoke, dramatically accelerates the growth of colon cancer cells inoculated into the subcutaneous space of mice. Our findings indicate that nicotine promotes tumor growth, at least in part, by enhancing tumor neovascularization.

* To whom correspondence should be addressed.
Tel: 81-3-3815-5411; Fax: 81-3-3814-0021
E-mail: msata-circ@umin.ac.jp

Materials and Methods

Study protocol All protocols involving experimental animals were in accordance with the institutional guidelines for animal care of the University of Tokyo. Male eight-week-old C57BL/6 mice were purchased from SLC Japan (Japan). Either vehicle (0.5% carboxymethylcellulose) or nicotine (20 mg/kg/day) was administered by gavage every day starting five days before tumor inoculation. The mice were anesthetized by intraperitoneal injection of 50 mg/kg of pentobarbital. We suspended 6×10^7 murine syngeneic colon cancer cells (CMT93, American Type Culture Collection,USA) in 0.1 ml of ECM gel (Sigma, USA) and injected them subcutaneously into the left flank fold of the mice, and measured tumor size with calipers every day. Tumor volume was calculated as width^2 × length × 0.52. The mice were killed at 11 days after implantation. The tumors were excised, fixed in methanol and embedded in paraffin. ROSA26 mice that express lacZ ubiquitously were originally purchased from Jackson Laboratory (Bar Harbor, ME). Bone marrow transplantation was performed as described (Sata *et al.*, 2002).

Measurement of capillary density Sections (5 μm) were deparaffinized and incubated with a rat monoclonal antibody against murine CD31 (clone MEC13.1, BD PharMingen, USA) (Sata *et al.*, 2001). Antibody distribution was visualized using the avidin-biotin-complex technique and Vector Red Chromogenic substrate (Vector Laboratories, Burlingame, CA), followed by counterstaining with hematoxylin. Capillaries were identified by positive staining for CD31 and morphology. Ten different fields from each tissue preparation were randomly selected, and capillaries counted. Capillary density is expressed as number of capillaries per square millimeter.

Detection of bone marrow-derived endothelial cells Tumors were embedded in OCT compound and snap frozen in liquid nitrogen. Frozen sections (5 μm) were fixed in formalin and stained with anti-lacZ rabbit polyclonal antibody (ICN, Aurora, OH) or anti-CD31 rat monoclonal antibody, followed by incubation with FITC-conjugated anti-rabbit Ig and rhodamine-conjugated anti-rat Ig secondary antibodies. Nuclei were counterstained with Hoechst 33258. The sections were observed with a confocal microscope (FLUOVIEW FV300, Olympus, Japan).

***In vitro* cell proliferation assay** CMT93 cells were maintained in Dulbecco's modified Eagle's medium supplemented with 10% fetal bovine serum. 7×10^4 cells were cultured per well of a 24-well culture plate in the presence or absence of nicotine for 24 h. and cell numbers counted after trypsinization.

***In vitro* VEGF production** CMT93 cells were cultured in 24-well culture plates in the presence or absence of nicotine for 24 h. VEGF concentration in the supernatant was measured using an anti-mouse VEGF ELISA kit (Quantikine M Colorimetric Sandwich ELISA kit, R&D systems, Minneapolis, MN).

Statistical analysis All results are expressed as means ± S.E.M. Means were statistically compared by ANOVA followed by Student's *t*-test. A value of $p < 0.05$ was considered to be significant.

Results

Promotion of tumor growth by nicotine To determine the effect of nicotine on tumor growth, we used a tumor implantation model; 6×10^7 murine syngeneic colon cancer cells (CMT93) were injected subcutaneously into the left flank fold of C57BL/6 mice, and the mice were treated with either nicotine (20 mg/kg/day, n = 6) or vehicle (n = 6). Tumor growth in the nicotine-treated group markedly exceeded that in the vehicle group ($p < 0.01$) (Fig. 1).

Effect of nicotine on carcinoma cell proliferation *in vitro* Next, we investigated whether nicotine directly stimulates proliferation of carcinoma cells. 7×10^4 CMT93 cells were cultured in the presence or absence of nicotine (10^{-12} to 10^{-4} M) for 24 h (n = 4 for each group). We found no significant difference in cell number between the groups (Fig. 2). On the other hand, nicotine (10^{-4} to 10^{-10} M) stimulated VEGF production by the CMT93 cells (data not shown) indicating that nicotine might promote tumor growth by enhancing vascularization.

Effects of nicotine on tumor vascularization To study the effect of nicotine on cancer-associated angiogenesis, we harvested tumors 11 days after implantation. Anti-

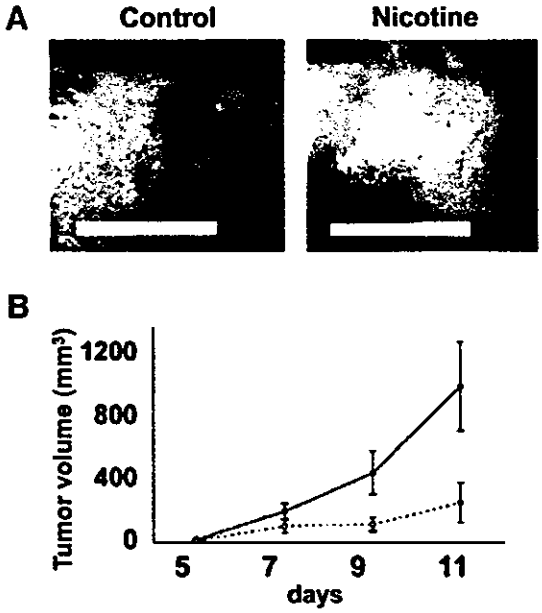

Fig. 1. Effect of nicotine on tumor growth *in vivo*. 6×10^7 murine syngeneic colon cancer cells (CMT93) were implanted subcutaneously into the left flank fold of C57BL/6 mice, and the mice received 20 mg/kg/day of nicotine or vehicle starting 5 days before implantation. **A.** Tumor appearance in the mice treated with nicotine or vehicle. Scale bar, 1 cm. **B.** Nicotine (closed circle, n = 6) or vehicle (open circle, n = 6) was administered to the mice. Tumor size was measured with calipers every day. Tumor volume was calculated as width^2 × length × 0.52.

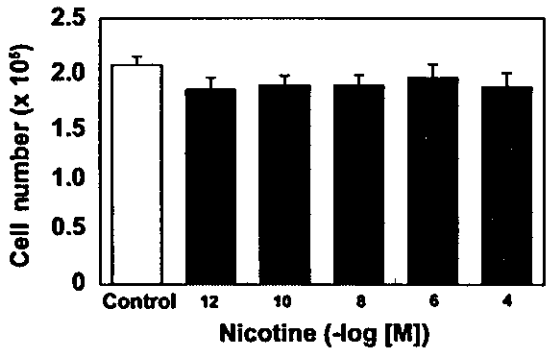

Fig. 2. Effect of nicotine on carcinoma cell proliferation *in vitro*. 7×10^4 CMT93 cells were cultured in the presence or absence of nicotine at the indicated concentrations. Numbers of cells were counted after 24 h (n = 4 for each group).

CD31 immunostaining revealed that many new vessels had formed (Fig. 3A); capillary density in the nicotine-treated mice was significantly higher than in the vehicle group (496 ± 29 versus 269 ± 25 capillaries/mm^2, $p < 0.01$) (n = 4 for each group) (Fig. 3B).

To study the potential contribution of bone marrow cells to the capillary formation we inoculated carcinoma cells into wild-type mice whose bone marrow had been replaced with that of ROSA26 mice, and the mice were

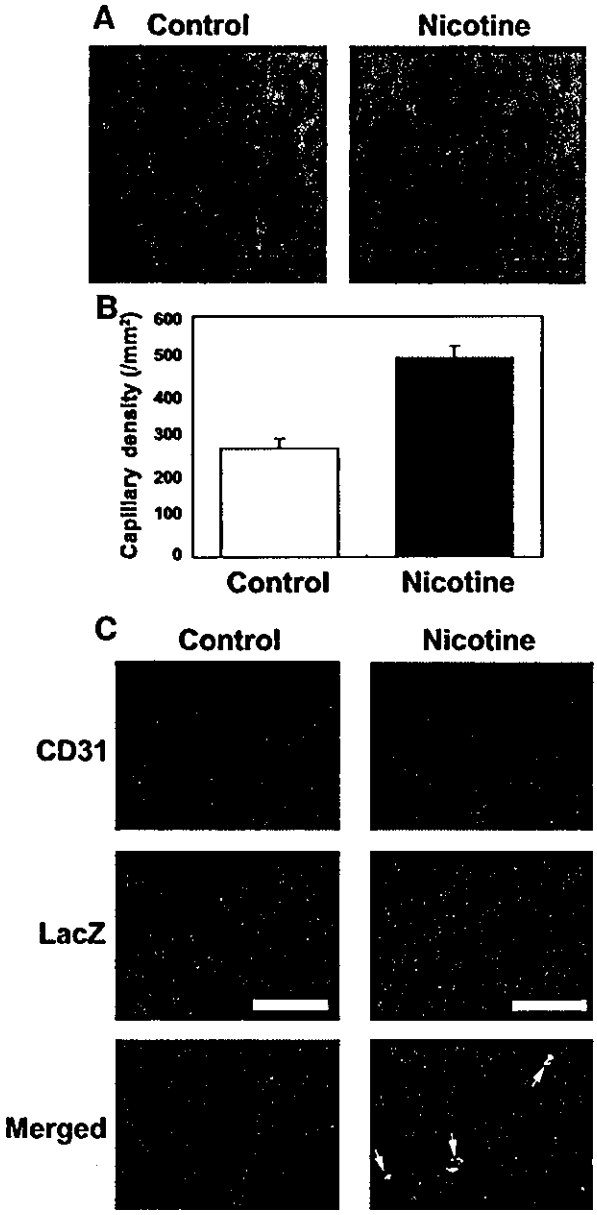

Fig. 3. Effect of nicotine on neovascularization in tumors. **A** and **B.** Tumors were harvested 11 days after implantation. Cross sections were stained for CD31 (A). Scale bar, 50 μm. Capillary density was measured (n = 4 for each group) (B). **C.** 1×10^7 CMT93 cells were implanted into wild-type mice whose bone marrow had been reconstituted with that of ROSA26 mice. The mice received vehicle or nicotine. At day 7, tumors were collected for immunofluorescence double staining to detect CD31 (red) and lacZ (green). Arrows indicate lacZ-positive endothelial cells. Bar, 50 μm.

treated with vehicle or nicotine for 7 d. We found CD31-positive endothelial cells that expressed lacZ, particularly in the tumors of the mice treated with nicotine (Fig. 3C). These results suggest that bone marrow derived cells can contribute to tumor neovascularization.

Discussion

The nicotine-derived nitrosamine, 4-(methylnitrosamino)-1-(3-pyridyl)-1 butanone, is one of the best known carcinogens among the many components of cigarette smoke (Hecht, 1999). On the other hand, it is generally believed that nicotine itself does not cause neoplastic transformation, and we also found that nicotine had no effect on the proliferation of cancer cells *in vitro*. However, it greatly increased the growth of inoculated tumors, and enhanced new blood vessel formation.

The production of new blood vessels involves two processes, vasculogenesis and angiogenesis (Carmeliet, 2000). Vasculogenesis is the *in situ* differentiation of mesodermal precursors to angioblasts that differentiate into endothelial cells to form the primitive capillary network. Angiogenesis is the sprouting of new capillaries from pre-existing blood vessels. Until recently, vasculogenesis was considered to be limited to early embryogenesis and postnatal neovascularization was thought to result from angiogenesis (Folkman and Shing, 1992). However, recent studies have identified circulating endothelial progenitor cells (Asahara *et al.*, 1997; 1999a; 1999b; Peichev *et al.*, 2000; Takahashi *et al.*, 1999) that play a critical role in physiological and pathological neovascularization (Asahara *et al.*, 1999a; Lyden *et al.*, 1999; 2001). In this study, we found that bone marrow-derived cells participated in new vessel development in tumors.

Nicotine acts via the nicotinic acetylcholine receptor (nAChR) that mediates fast synaptic transmission (Pontieri *et al.*, 1996). Endothelial cells also express nAChR and nicotine stimulates their proliferation *in vitro* (Heeschen *et al.*, 2001; Villablanca, 1998). Nicotine also stimulates vascular endothelial cell growth factor (VEGF) expression in endothelial cells (Conklin *et al.*, 2002), and we also found that nicotine stimulated VEGF production in tumor cells and that it enhanced tumor-associated angiogenesis. Taken together, these findings suggest that nicotine up-regulates VEGF expression by cancer cells and augments tumor-associated angiogenesis and vasculogenesis, leading to enhanced tumor growth.

In summary, we found that nicotine promotes tumor growth, at least in part, by stimulating neovascularization. Our findings provide additional insight into the mechanism by which smoking enhances the development of cancers.

Acknowledgments This study was supported in part by grants from the Ministry of Education, Culture, Sports, Science and Technology (15039213, 15390241, and 15659180), the Ministry of Health, Labor and Welfare, and the Motor Vehicle Trust Fund for Research on Heart Diseases (Dr. Sata).

References

Asahara, T., Murohara, T., Sullivan, A., Silver, M., van der Zee, R., Li, T., Witzenbichler, B., Schatteman, G., and Isner, J. M. (1997) Isolation of putative progenitor endothelial cells for angiogenesis. *Science* **275**, 964–967.

Asahara, T., Masuda, H., Takahashi, T., Kalka, C., Pastore, C., Silver, M., Kearne, M., Magner, M., and Isner, J. M. (1999a) Bone marrow origin of endothelial progenitor cells responsible for postnatal vasculogenesis in physiological and pathological neovascularization. *Circ. Res.* **85**, 221–228.

Asahara, T., Takahashi, T., Masuda, H., Kalka, C., Chen, D., Iwaguro, H., Inai, Y., Silver, M., and Isner, J. M. (1999b) VEGF contributes to postnatal neovascularization by mobilizing bone marrow-derived endothelial progenitor cells. *EMBO J.* **18**, 3964–3972.

Bartecchi, C. E., MacKenzie, T. D., and Schrier, R. W. (1994) The human costs of tobacco use. *N. Engl. J. Med.* **330**, 907–912.

Carmeliet, P. (2000) Mechanisms of angiogenesis and arteriogenesis. *Nat. Med.* **6**, 389–395.

Conklin, B. S., Zhao, W., Zhong, D. S., and Chen, C. (2002) Nicotine and cotinine up-regulate vascular endothelial growth factor expression in endothelial cells. *Am. J. Pathol.* **160**, 413–418.

Folkman, J. (1990) What is the evidence that tumors are angiogenesis dependent? *J. Natl. Cancer Inst.* **82**, 4–6.

Folkman, J. (1995) Seminars in medicine of the Beth Israel Hospital, Boston. Clinical applications of research on angiogenesis. *N. Engl. J. Med.* **333**, 1757–1763.

Folkman, J. and Shing, Y. (1992) Angiogenesis. *J. Biol. Chem.* **267**, 10931–10934.

Hecht, S. S. (1999) Tobacco smoke carcinogens and lung cancer. *J. Natl. Cancer Inst.* **91**, 1194–1210.

Heeschen, C., Jang, J. J., Weis, M., Pathak, A., Kaji, S., Hu, R. S., Tsao, P. S., Johnson, F. L., and Cooke, J. P. (2001) Nicotine stimulates angiogenesis and promotes tumor growth and atherosclerosis. *Nat. Med.* **7**, 833–839.

Lyden, D., Young, A. Z., Zagzag, D., Yan, W., Gerald, W., O'Reilly, R., Bader, B. L., Hynes, R. O., Zhuang, Y., Manova, K., and Benezra, R. (1999) Id1 and Id3 are required for neurogenesis, angiogenesis and vascularization of tumour xenografts. *Nature* **401**, 670–677.

Lyden, D., Hattori, K., Dias, S., Costa, C., Blaikie, P., Butros, L., Chadburn, A., Heissig, B., Marks, W., Witte, L., Wu, Y., Hicklin, D., Zhu, Z., Hackett, N. R., Crystal, R. G., Moore, M. A., Hajjar, K. A., Manova, K., Benezra, R., and Rafii, S. (2001) Impaired recruitment of bone-marrow-derived endothelial and hematopoietic precursor cells blocks tumor angiogenesis and growth. *Nat. Med.* **7**, 1194–1201.

O'Reilly, M. S., Holmgren, L., Shing, Y., Chen, C., Rosenthal, R. A., Moses, M., Lane, W. S., Cao, Y., Sage, E. H., and Folkman, J. (1994) Angiostatin: a novel angiogenesis inhibitor that mediates the suppression of metastases by a Lewis lung carcinoma. *Cell* **79**, 315–328.

Peichev, M., Naiyer, A. J., Pereira, D., Zhu, Z., Lane, W. J., Williams, M., Oz, M. C., Hicklin, D. J., Witte, L., Moore, M. A., and Rafii, S. (2000) Expression of VEGFR-2 and AC133 by circulating human CD34(+) cells identifies a population of functional endothelial precursors. *Blood* **95**, 952–958.

Pontieri, F. E., Tanda, G., Orzi, F., and Di Chiara, G. (1996) Effects of nicotine on the nucleus accumbens and similarity to those of addictive drugs. *Nature* **382**, 255–257.

Sata, M., Nishimatsu, H., Suzuki, E., Sugiura, S., Yoshizumi, M., Ouchi, Y., Hirata, Y., and Nagai, R. (2001) Endothelial nitric oxide synthase is essential for the HMG-CoA reductase inhibitor cerivastatin to promote collateral growth in response to ischemia. *FASEB J.* **15**, 2530–2532.

Sata, M., Saiura, A., Kunisato, A., Tojo, A., Okada, S., Tokuhisa, T., Hirai, H., Makuuchi, M., Hirata, Y., and Nagai, R. (2002) Hematopoietic stem cells differentiate into vascular cells that participate in the pathogenesis of atherosclerosis. *Nat. Med.* **8**, 403–409.

Takahashi, T., Kalka, C., Masuda, H., Chen, D., Silver, M., Kearney, M., Magner, M., Isner, J. M., and Asahara, T. (1999) Ischemia- and cytokine-induced mobilization of bone marrow-derived endothelial progenitor cells for neovascularization. *Nat. Med.* **5**, 434–438.

Villablanca, A. C. (1998) Nicotine stimulates DNA synthesis and proliferation in vascular endothelial cells *in vitro*. *J. Appl. Physiol.* **84**, 2089–2098.

Available online at www.sciencedirect.com
SCIENCE DIRECT®
Transplant Immunology 12 (2003) 41–48
Transplant Immunology
www.elsevier.com/locate/trim

Simultaneous blockade of co-stimulatory signals, CD28 and ICOS, induced a stable tolerance in rat heart transplantation

Lei Guo[a,b], Masayuki Fujino[a], Hiromitsu Kimura[a], Naoko Funeshima[a], Yusuke Kitazawa[a], Yasushi Harihara[b], Katsunari Tezuka[c], Masatoshi Makuuchi[b], Seiichi Suzuki[a], Xiao-Kang Li[a,*]

[a]*Laboratory of Transplantation Immunology, Department of Innovative Surgery, National Research Institute for Child Health and Development, 3-35-31 Taishido, Setagaya-ku, Tokyo 154-8567, Japan*
[b]*Department of Artificial Organ and Transplantation Surgery, Graduate School of Medicine and Faculty of Medicine, University of Tokyo, Tokyo, Japan*
[c]*Pharmaceutical Frontier Research Laboratories, JT Inc., Yokohama, Japan*

Received 2 December 2002; accepted 24 January 2003

Abstract

An inducible co-stimulator (ICOS), a recently identified co-stimulatory receptor with a close structural homology of CD28 and CTLA4, is expressed on activated T cells. anti-ICOS antibody was demonstrated to be effective on prolongation of graft survival after liver transplantation in rats. In this study, we investigated the potency of tolerance induction using the antibody combined with a recombinant adenovirus vector containing CTLA-4Ig cDNA (AdCTLA-4Ig) in rat heart transplantation model. Using a DA-to-Lewis rat heart transplantation model, an anti-rat ICOS antibody and AdCTLA-4Ig were simultaneously administered i.v. into recipients. The tissue specimens from the grafts were removed on various days after transplantation for histological evaluation. Donor-strain skin and heart grafts, and third-party heart allografts were challenged in the recipients with a long-term surviving graft. Splenocytes from the tolerance-induced recipients were used for adoptive transfer study. Anti-ICOS antibody alone did not prolong the survival of heart allograft. AdCTLA-4Ig monotherapy significantly prolonged the survival of heart allograft (Group 4). With a combination of Anti-ICOS antibody and AdCTLA-4Ig, all recipients were resulted in a long-term allograft acceptance for more than 200 days (Group 8). When challenged donor-strain skin grafts in the tolerant rats of Group 4, the skin was rejected, which also lead to a rejection of primary heart allografts. The recipients in Group 8 also rejected donor-strain skin grafts with no rejection of the primary heart grafts. These recipients accepted secondary heart grafts from donor-strain but not third-party. In Group 8 long-term survival recipients showed a high population of $CD4^+CD25^+$ regulatory T cell in peripheral blood, and in adoptive transfer study subtraction of these $CD4^+CD25^+$ T cells accelerate the rejection of heart graft in secondary irradiated recipients. The present results demonstrated that anti-ICOS antibody combined with AdCTLA-4Ig potently induces a stable immune tolerance after heart allografting in rat, which is mediated by the induction of $CD4^+CD25^+$ regulatory T cells. This strategy may be attractive for clinical employment to induce transplantation tolerance.

Keywords: Co-stimulatory pathway; Tolerance; Liver transplantation; Regulatory T cell

1. Introduction

Co-stimulatory signals via CD80–CD28 and CD40–CD154 pathways play a crucial role in T cell activity. Each of these two pathways appears to serve as a critical and independent regulator of the T cell-dependent immune response. Recently, much attention has been paid to the co-stimulation blockade in the transplant field. Blockade of CD80–CD28 or CD40–CD154 interaction by administration of a soluble inhibitory fusion protein CTLA-4Ig and monoclonal antibody to CD154, either alone or in combination, resulted in prolonged allograft survival in rodent models [1–4]. CD28 and CD154 have been investigated in primary T-cell activation [5,6], however, these molecules appear to be far less important in the generation and maintenance of secondary T-cell response [7].

*Corresponding author. Tel.: +81-3-3416-0181; fax: +81-3411-7309.
E-mail address: sri@nch.go.jp (X.-K. Li).

0966-3274/03/$ - see front matter © 2003 Elsevier Science B.V. All rights reserved.
doi:10.1016/S0966-3274(03)00016-9

An inducible co-stimulator (ICOS), a new member of co-stimulatory molecules, was recently identified as a structural homology of CD28 and CTLA-4. Unlike CD28, ICOS is not constitutively expressed on T cells, and induced after their activation [8]. ICOS does not interact with the ligands for CD28 and CTLA4 (B7.1 and B7.2), but interacts with its own ligand originally called B7h [9], B7RP-1 [10], GL50 [11], or LICOS [12]. This molecule maintains or modulates immune responses in primed and memory T-cells [13]. The stimulation of ICOS in response to TCR activation, augmented T-cell proliferation [8]. Coyle et al. suggested that ICOS is an important co-stimulatory receptor for the recently activated cells as well as effector cells; a blockade of ICOS was effective in suppressing the function of recently activated helper T-cells, resulting in the inhibition of IL-4 and IFN-γ production. As opposed to CD80–CD28, ICOS–B7RP-1 interaction may be required at a later stage of the immune response and predominate over CD28 for inducing secondary immune response [14].

Co-stimulatory blockade successfully prolonged graft survival in various rodent allograft models, including heart, liver, islet, kidney, lung and bone marrow transplantation [15–17]. In rat liver transplantation, we have successfully prolonged recipient survival in association with a reduction of ICOS expression of intragraft-infiltrating cells and an inhibition of T-cells activation by using anti-ICOS antibody [18]. Ozkaynak et al. showed a similar result in which anti-ICOS antibody combined with cyclosporin A or anti-CD154 antibody prevented an occurrence of chronic rejection and induced a long-term acceptance of cardiac grafts in mice, indicating that the ICOS-B7RP-1 pathway is important in the development of acute and chronic allograft rejections [19]. However, the mechanism and tolerogenic potential of ICOS blockade is not clear yet.

In the present study, we aimed to evaluate the potential and study the mechanism of a therapy using a CTLA-4Ig-carrying adenovirus vector (AdCTLA-4Ig) in combination with anti-ICOS antibody for tolerant induction in rat heart allografting. We show herein that when combined with AdCTLA-4Ig, a single administration of anti-ICOS antibody potentially induced a stable transplantation tolerance. The key mechanism of the combination therapy in the induction and maintenance of tolerance is associated with the induction of regulatory T cells.

2. Objective

In the present study, we aimed to evaluate the potential and studied the mechanism of a therapy using a CTLA-4Ig-carrying adenovirus vector (AdCTLA-4Ig) in combination with anti-ICOS antibody for tolerant induction in rat heart allografting.

3. Materials and methods

3.1. Adenoviral vector

The adenovirus containing the expression cassette for human CTLA-4Ig gene or *Escherichia coli* β–galactosidase gene (LacZ) was constructed by homologous recombination between the expression cosmid cassette (pAdex/CAhCTLA4Ig) [20] and the parental virus genome [21]. The recombinant viruses were subsequently propagated with 293 cells. The prepared vector solutions were stored at −80 °C. The adenovirus contains CTLA-4Ig gene and those containing LacZ were termed as AdCTLA-4Ig and AdLacZ, respectively.

3.2. Animals and antibody

We used adult male Lewis ($RT1^l$) rats as recipients, and DA ($RT1^a$) or BN ($RT1^n$) rats as donors. The animals weighed 210–250 g and were maintained under a standard condition with feeding rodent food and water, according to the principle of laboratory animal care and the guide for the care and use of laboratory animals in our institution. Mouse monoclonal IgG1 to rat ICOS (JTT.1, anti-ICOS mAb) was generated by the method described previously [22].

3.3. Heart and skin transplantation model

For primary heart transplantation, DA hearts were transplanted into abdominal cavity of Lewis recipients by the method reported by Ono and Lindsey [23]. The recipients received intravenously a single dose of anti-ICOS mAb at 1 mg/kg and/or AdCTLA-4Ig at 10^9 plaque-forming units (PFUs) immediately after transplantation. The recipients without any treatment and those with AdLacZ-administration or control IgG were served as controls. The completion of graft rejection was defined as a cessation of graft palpitation and the rejection was histologically confirmed by mononuclear cell infiltration and myocyte necrosis in the graft sections with hematoxylin and eosin (HE)-staining.

The recipients with a graft survived for more than 100 days were transplanted a full-thickness donor-type skin graft to the lateral thoracic wall. No further immunosuppression was given after skin grafting. The day of the skin graft survival was determined as the time when the viable area reduced to less than 10% of the graft. In three of Group 8 recipients with a rejection of donor-type skin, secondary hearts from specific donor (DA) were grafted into the cervical location using the cuff technique, essentially as described previously [24], on 300 days after primary heart grafting. In addition, three of the Group 8 recipients with no skin grafting received secondary heart grafts from third-party (BN) rats on 300 days after grafting.

Table 1
Survival of primary heart grafts

Group	Treatment	n	Survival	Median	P*
Syngenic					
1	No-treatment	4	>300×4	>300	
Allogenic					
2	No-treatment	10	5×3, 6×7	6	
3	AdLacZ	7	6×4, 7×3	6	
4	AdCTLA-4Ig	11	40, 42, 56, 62, 64, 65, 68, 109, >100[a,c], >140×2[a,c]	64	<0.001
5	Anti-ICOS	7	5×2, 6×5	6	
6	AdLacZ+Anti-ICOS	5	5×3, 6×2	6	
7	AdCTLA-4Ig+Control Ig	5	26, 53, 61, 67, 98	61	<0.001
8	AdCTLA-4Ig+Anti-ICOS	12	>300×3[a,b], >200×3[a,c], >300×3[d], >200×3[e]	>300	<0.001

[a,b,c,d] and [e] were recipients used for primary donor-strain skin grafting, secondary donor heart grafting, sacrificed for histological study, third party (BN) heart grafting, and FACS sorting, respectively.

3.4. Splenocyte preparation and adoptive transfer

Spleens were harvested from three recipients, when the allograft survival reached 200 days in Group 8, and naïve Lewis rats. We gently grounded these spleens with frosted objective slides in PBS for single cell-suspension preparation. Following lysing of erythrocytes with RBC lysis buffer (Sigma, St. Louis, MO, USA), the splenocytes were washed three times. For adoptive transfer study, the splenocytes were intravenously administered at 5×10^7 cells into 7.5 Gy-irradiated Lewis rats (secondary recipients), and thereafter heart transplantation from specific donors was performed in the abdominal cavity. For sorting $CD4^+CD25^+$ T cell fraction, the splenocytes were stained with PE-conjugated anti-CD25 antibody (α-chain of IL-2 receptor, Pharmingen) for 15 min, and then washed and resuspended in 80 μl of sorting buffer per 10^7 total cells. We added 20 μl of MACS-anti-PE microbeads (Miltenyi Biotec GmbH, Germany) to this cell suspension and incubated for 15 min in refrigerator at 4 °C. For cell separation, 10^8 cells were suspended in 500 μl of buffer, and applied onto the column of Auto-MACS (Miltenyi Biotec GmbH). After passage of the negative cells through the column, we collected $CD25^+$ cells and stained the cells with FITC-conjugated anti-CD4 antibody (Pharmingen) for FACS sorting (EPICS ALTRA, Beckman Coulter, Miami, FL, USA). The cells without $CD4^+CD25^+$ T cell fraction were collected and subjected to the same process as described above. Spleens from naïve Lewis rat were subjected to the same protocol using as controls.

3.5. Histological studies

Heart grafts were harvested on various days after donor strain skin grafting in each group. The samples were formalin-fixed and embedded in paraffin for HE staining.

3.6. Flow cytometric analysis

The peripheral blood from recipients with a long-term surviving graft (over 300 days) and that from syngeneic and naïve Lewis rats were collected without killing and overlaid on Ficoll Isopaque. After centrifugation, the cells of the interface layer were harvested and suspended at 2×10^6/ml in PBS. The cells (2×10^6) were incubated at 4 °C for 30 min with a saturating concentration of PE-conjugated anti-rat CD4 antibody (W3/25, Pharmingen) in combination with FITC-conjugated anti-rat CD25 antibody (OX-39, Pharmingen) diluted with PBS containing 1% fetal calf serum. After washing, the cells were resuspended in 1 ml of PBS, followed by analysis with flow cytometry (FACScan, Becton Dickinson). The dead cells were excluded from the analysis using propidium iodide fluorescence.

3.7. Statistics

A statistical evaluation for graft survival was performed using Kaplan–Meier's test. The difference in population of T cells was analyzed for significance using Student's *t*-test.

4. Results

4.1. Primary heart allograft survival

As shown in Table 1, no significant prolongation of allograft survival was obtained in the recipients treated with AdLacZ (Group 3), a single dose of anti-ICOS antibody (Group 5), and their combination (Group 6), comparing to the non-treated allogeneic group (Group 2). In contrast, the treatment with AdCTLA-4Ig (Group 4) significantly prolonged the survival of primary heart allografts (64 days in median), and a long-term graft acceptance (>100 days) was observed in four out of

Table 2
Subsequent engraftment of donor-strain skin or heart in long-term graft-surviving recipients

Groups	n	Skin graft reject	Primary heart reject*	Secondary heart reject
Naive Lewis (control)	10	10/10		
Group 4	3	3/3	3/3	
Group 8	6	6/6	0/6	0/3

* Primary heart was rejected after skin rejection.

11 recipients. Furthermore, anti-ICOS antibody combined with AdCTLA-4Ig (Group 8) resulted in an indefinite acceptance (>300 days) of primary heart grafts in all recipients. However, AdCTLA-4Ig combined with Control Ig (Group 7) could not further improve survival of the heart graft compared with Group 8.

4.2. Skin and second heart graft in long-term graft-accepting recipients

The long-term graft-accepting recipients in Group 4 and Group 8 received the skin grafts from donor strain on 140–150 days after heart transplantation. As shown in Table 2, all skin grafts in Groups 4 and 8 were completely rejected. In accordance with skin rejection, the primary heart grafts in Group 4 were also rejected, but not those in Group 8. The skin-graft rejection in Group 4 and Control was completed by 12 days, although that in Group 8 was accomplished with a delayed process (approx. 16 days). Interestingly, the long-term graft-surviving recipients in Group 8 indefinitely accepted the secondary heart grafts from donor-strain, despite the complete rejection of donor skin graft. In addition, the primary heart grafts in all of those recipients continued to survive throughout the experiment.

4.3. Third-party heart grafting

BN hearts were transplanted as a third-party graft into the recipients of Group 8. These recipients rejected the BN hearts as similar time course as naïve Lewis rats, although the primary heart grafts continued to beat well throughout the experiment (Table 3).

4.4. Histological studies

The sections of the long-surviving grafts from Groups 4 and 8 after donor-strain skin grafting were stained with HE and observed with light microscopy. In Group 4, an extensive perivascular accumulation of mononuclear cells was seen, while evidence of myocyte necrosis and bleeding were noted in the rejected heart graft after skin grafting (Fig. 1A). A slight perivascular accumulation of mononuclear cells with normal tissue architecture was observed on 200 days even after a donor-skin rejection in Group 8 (Fig. 1B).

4.5. Population of $CD25^+CD4^+$T cells in peripheral lymphocytes

We performed FACS analysis using the peripheral lymphocytes prepared from long-term graft surviving recipients over 300 days in Group 8, syngeneic recipients (Group 1) and naïve Lewis rats. The proportion of $CD4^+CD25^+$ T cells was 11.9% (means) in Group 8, which was significantly higher than in Group 1 (means 7.1%) and naive Lewis rats (means 8.1%) (Fig. 2).

4.6. Adoptive transfer

Some recipients in Group 8 were used for adoptive transfer study 200 days after primary heart grafting. After whole body irradiation (7.5 Gy) of Lewis rats (secondary recipients), prepared splenocytes (5×10^7) from the recipients of Group 8 and naïve Lewis rats with or without subtraction of the $CD4^+CD25^+$ T cell fraction were transferred, and thereafter donor-strain hearts were transplanted. As shown in Table 4, the recipients received splenocytes from naïve Lewis rats rejected donor-strain hearts on 13.7 days (mean) after grafting. Subtraction of $CD4^+CD25^+$ T cells from naïve Lewis splenocytes did not significantly affect the survival of heart graft (mean 14.3 days). However, three secondary recipients received Group 8 splenocytes significantly prolonged the survival of heart graft to 24.5 days (mean), and those received the cells without $CD4^+CD25^+$ T cell fraction resulted in no significant prolongation of graft survival (mean 15.7 days).

5. Discussion

Blocking T-cell costimulatory signals has successfully inhibited lymphocyte responses in autoimmune disease and transplantation immunity [6]. In particular, blockade of CD28–CD80 interaction by CTLA-4Ig prolonged survival of vascularized grafts and frequently led to permanent graft acceptance in animal models including kidney and islet allotransplantations. However, in rat heart allografting, an indefinite graft survival using

Table 3
Subsequent engraftment of third-party heart allografts in Group 8 recipients and naïve Lewis rats

Recipient	n	Third party heart reject	Primary heart reject
Naive Lewis (Control)	5	5/5	
Group 8	3	3/3	0/3

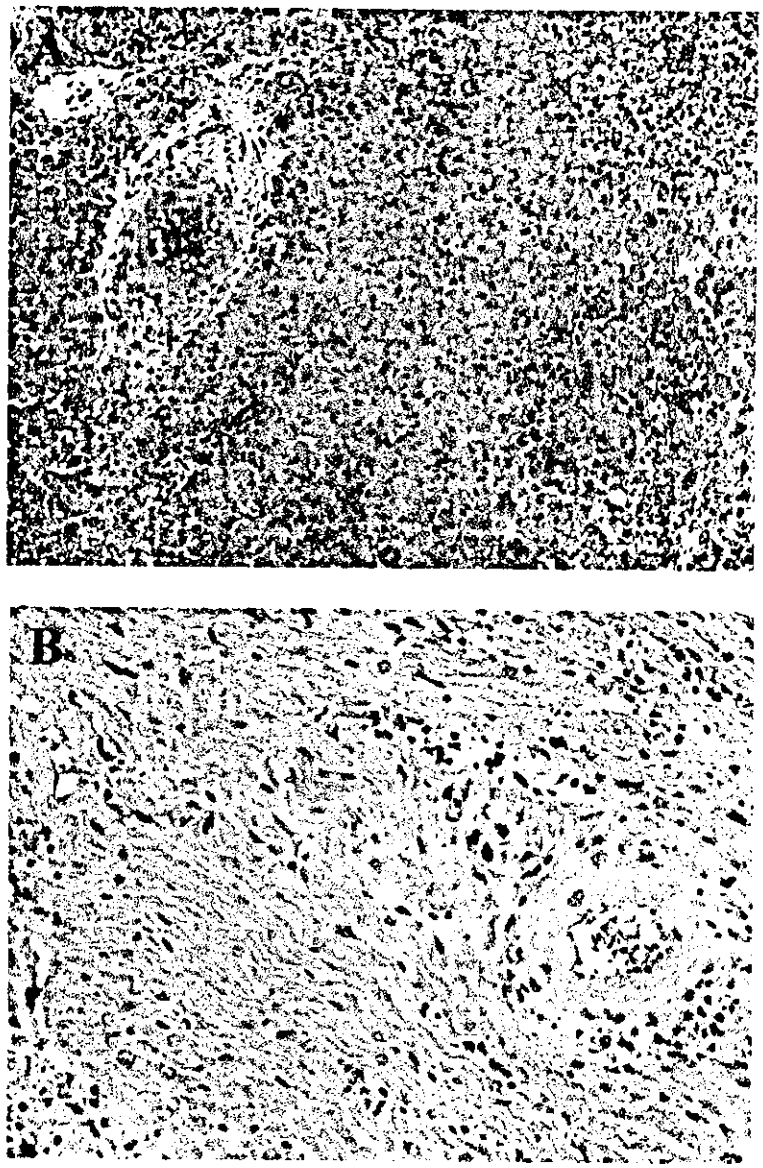

Fig. 1. Histological finding in long-surviving grafts: (A) an extensive perivascular accumulation of mononuclear cells with a clear evidences of myocyte necrosis and bleeding were seen in Group 4 after skin grafting; and (B) a normal tissue architecture with little infiltration of mononuclear cells was observed on day 200 even after a donor-skin rejection in Group 8.

CTLA-4Ig was only achieved by simultaneous administration of donor cells [25], or anti-CD40L antibody [3], anti-CD4 antibody [26]. In this study, an administration of AdCTLA-4Ig alone did not induce a stable tolerance, even though the recipients were treated with a high titer of the vector; only four of the 11 heart allografts survived more than 100 days. With the same titer, we successfully induced an indefinite survival of liver allografts in rats (unpublished data). Although a single dose of anti-ICOS mAb did not improve the survival of heart allografts, the antibody in combination with AdCTLA-4Ig resulted in more stable tolerance than AdCTLA-4Ig-alone. Our results suggested that CTLA-4Ig acts to inhibit the immune response during early phase after grafting, and administration of anti-ICOS mAb in the early phase of transplantation in combination with CTLA-4Ig plays an important role in tolerant induction and maintenance.

When challenged with a donor-strain skin graft, the tolerant recipients completely rejected the skin. The skins grafted in Group 4 recipients were rejected similar to those in the control group. However, AdCTLA-4Ig plus anti-ICOS mAb treated recipients delayed the rejection. These data indicated that the heart-graft acceptance in the present combination therapy was not associated with clonal anergy or deletion, but with an active mechanism such as an activation of the immunoregulatory system.

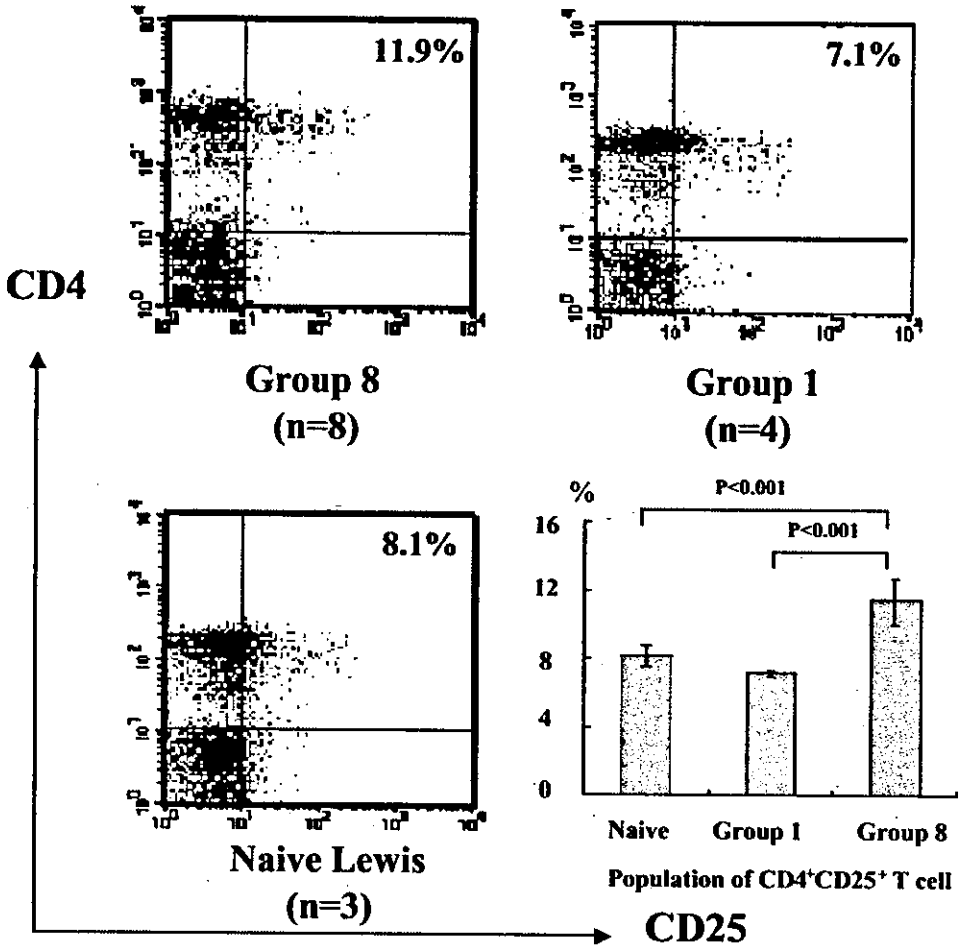

Fig. 2. FACS analysis in peripheral lymphocytes from Group 8. The proportion of $CD4^+CD25^+$ T cells was 11.9% in mean in Group 8, which was significantly higher than that in Group 1 (7.1% in mean) and naïve Lewis rats (8.1% in mean). The lymphocytes from Group 1 and Group 8 were prepared 300 days after primary heart grafting.

Despite the rejection of skin allografts, the recipients in Group 8 did not reject the primary heart graft and accepted the secondary heart without any additional immuno-suppressive therapy. In some models of tolerance induction toward vascularized organs, a dichotomy has also been described between rejection of the donor skin graft and acceptance of the secondary organ graft. Skin graft was found to be far more susceptible to rejection than the heart graft [27]. A relatively small numbers of donor-reactive T cells that escaped from suppressive mechanisms may be insufficient to adversely affect a resistant graft such as a heart, while these T-cells may be sufficient in number to reject a susceptible graft such as skin. In addition, we have demonstrated that the effective serum concentration of CTLA-4Ig continued only 1 month after its gene transfer [20]. It was also shown that a half-life of anti-ICOS antibody is 1.5 days (unpublished data). Thus, the acceptance of secondary heart grafts in Group 8 is not due to the presence of CTLA-4Ig or anti-ICOS mAb, it might be

Table 4
Graft survival in irradiated Lewis rats transferred with splenocytes from Group 8 and naïve Lewis rats

Transfer cells	*n*	Survival (days)	Mean	*P**
Naïve Lewis	10	12×3, 14×4, 15×3	13.7	
Naïve Lewis without $CD4^+CD25^+$	3	14×2, 15	14.3	
Group 8	3	23×2, 26	24	<0.001
Group 8 without $CD4^+CD25^+$	3	14, 15, 18	15.7	

Subtraction of $CD4^+CD25^+$ T cell fraction was performed by Auto-MACS with anti-CD25 antibody, and by FACS with anti-CD4 antibody.
* When compared with other three groups.

through an accomplishment of an immuno-regulative mechanism. In addition, the third-party grafts in Group 8 were readily rejected, demonstrating the induced tolerance was donor-specific.

$CD4^+CD25^+$ T cells have been reported as important immunoregulatory cells that are essential for T cell-homeostasis and prevent autoimmunity [28–31]. Thornton and Shevach showed that $CD4^+CD25^+$ immunoregulatory T cells suppress polyclonal T cell activation in vitro by inhibiting IL-2 production. We accessed the population of the $CD4^+CD25^+$ T cell subset in peripheral blood lymphocytes in the tolerant recipients and an increased number of these cells were observed in Group 8. To further study the role of $CD4^+CD25^+$ T cells in the immune regulation of tolerance in Group 8, an adoptive transfer of splenocytes was performed to the irradiated secondary recipients. The results revealed that splenocytes containing a $CD4^+CD25^+$ T cell fraction from Group 8 significantly prolonged survival of heart grafts; in contrast, subtraction of $CD4^+CD25^+$ T cell fraction from the splenocytes resulted in no significant prolongation of the graft survival. Therefore, we considered that $CD4^+CD25^+$ T cells induced by the present combination therapy actively inhibited the reactivity of donor-reactive T cells. These suggested that in contrast to the action of CTLA-4Ig, the anti-ICOS mAb might play an important role in the induction of $CD4^+CD25^+$ regulatory T cells for maintaining the tolerance.

Another possible mechanism that is more likely involved in this transplantation tolerance is modulation of ICOS co-stimulation with anti-ICOS mAb, which affects the potency of the T-cell activation signal, which leads to more effective signal transduction, a change in the balance of transcription factor induction and Th2 differentiation, which had been demonstrated to be important in tolerant induction and maintenance. However, we did not observe any remarkable change in the cytokine profile of peripheral lymphocytes (data not show). It seems that Th2 deviation may not be an important mechanism for tolerance in the present model. Ozkaynak et al. suggested that a prolonged survival of the cardiac allograft by inhibition of the ICOS signal, either by blocking mAb or using ICOS-deficient mice, was associated with a reduced production of IFN-γ and IL-10 [19]. In addition, T cells from ICOS-deficient mice showed a defect in IL-4 production [8]. It was also demonstrated that prolonged liver and heart allograft survivals by anti-ICOS antibody alone or in combination with a blockade of CD40 ligand, was strongly associated with an inhibition of the Th1 response [18,19].

As a result, this study and our previous findings suggest that anti-ICOS mAb treatment play an important role in primary immune inhibition as well as the maintenance stage of transplantation tolerance. Anti-ICOS mAb combined with AdCTLA-4Ig induced a stable and long-term allograft acceptance, which associated with a high population of $CD4^+CD25^+$ T lymphocytes by an immunoregulatory mechanism.

Acknowledgments

The authors thank Mr T. Sakai for his technique support. This study was supported by Research Grants from the Ministry of Health, Labour and Welfare of Japan (12-KO-2, Millennium Project H12-Saisei-016), and a Grant-in-Aid (no. 10307030) and a Grant for Organized Research Combination System from the Ministry of Education, Culture, Sports, Science and Technology of Japan.

References

[1] Kenyon NS, Chatzipetrou M, Masetti M, et al. Long-term survival and function of intrahepatic islet allografts in rhesus monkeys treated with humanized anti-CD154. Proc Natl Acad Sci USA 1999;96(14):8132–8137.
[2] Kirk AD, Harlan DM, Armstrong NN, et al. CTLA4-Ig and anti-CD40 ligand prevent renal allograft rejection in primates. Proc Natl Acad Sci USA 1997;94(16):8789–8794.
[3] Larsen CP, Elwood ET, Alexander DZ, et al. Long-term acceptance of skin and cardiac allografts after blocking CD40 and CD28 pathways. Nature 1996;381(6581):434–438.
[4] Turka LA, Linsley PS, Lin H, et al. T-cell activation by the CD28 ligand B7 is required for cardiac allograft rejection in vivo. Proc Natl Acad Sci USA 1992;89(22):11102–11105.
[5] Laning JC, Deluca JE, Isaacs CM, Hardin-Young J. In vitro analysis of CD40–CD154 and CD28–CD80/86 interactions in the primary T-cell response to allogeneic 'nonprofessional' antigen presenting cells. Transplantation 2001;71(10):1467–1474.
[6] Lenschow DJ, Walunas TL, Bluestone JA. CD28/B7 system of T cell costimulation. Annu Rev Immunol 1996;14:233–258.
[7] Howland KC, Ausubel LJ, London CA, Abbas AK. The roles of CD28 and CD40 ligand in T cell activation and tolerance. J Immunol 2000;164(9):4465–4470.
[8] Hutloff A, Dittrich AM, Beier KC, et al. ICOS is an inducible T-cell co-stimulator structurally and functionally related to CD28. Nature 1999;397(6716):263–266.
[9] Swallow MM, Wallin JJ, Sha WC. B7h, a novel costimulatory homolog of B7.1 and B7.2, is induced by TNFalpha. Immunity 1999;11(4):423–432.
[10] Yoshinaga SK, Whoriskey JS, Khare SD, et al. T-cell co-stimulation through B7RP-1 and ICOS. Nature 1999;402(6763):827–832.
[11] Ling V, Wu PW, Finnerty HF, et al. Cutting edge: identification of GL50, a novel B7-like protein that functionally binds to ICOS receptor. J Immunol 2000;164(4):1653–1657.
[12] Brodie D, Collins AV, Iaboni A, et al. LICOS, a primordial costimulatory ligand? Curr Biol 2000;10(6):333–336.
[13] Yoshinaga SK, Zhang M, Pistillo J, et al. Characterization of a new human B7-related protein: B7RP-1 is the ligand to the co-stimulatory protein ICOS. Int Immunol 2000;12(10):1439–1447.
[14] Coyle AJ, Lehar S, Lloyd C, et al. The CD28-related molecule ICOS is required for effective T cell-dependent immune responses. Immunity 2000;13(1):95–105.

[15] Sayegh MH, Turka LA. The role of T-cell costimulatory activation pathways in transplant rejection. N Engl J Med 1998;338(25):1813–1821.

[16] Tran HM, Nickerson PW, Restifo AC, et al. Distinct mechanisms for the induction and maintenance of allograft tolerance with CTLA4-Fc treatment. J Immunol 1997;159(5):2232–2239.

[17] Wallace PM, Johnson JS, MacMaster JF, Kennedy KA, Gladstone P, Linsley PS. CTLA4Ig treatment ameliorates the lethality of murine graft-versus-host disease across major histocompatibility complex barriers. Transplantation 1994;58(5):602–610.

[18] Guo L, Li XK, Funeshima N, et al. Prolonged survival in rat liver transplantation with mouse monoclonal antibody against an inducible costimulator (ICOS). Transplantation 2002;73(7):1027–1032.

[19] Ozkaynak E, Gao W, Shemmeri N, et al. Importance of ICOS-B7RP-1 costimulation in acute and chronic allograft rejection. Nat Immunol 2001;2(7):591–596.

[20] Kita Y, Li XK, Ohba M, et al. Prolonged cardiac allograft survival in rats systemically injected adenoviral vectors containing CTLA4Ig-gene. Transplantation 1999;68(6):758–766.

[21] Kass-Eisler A, Falck-Pedersen E, Alvira M, et al. Quantitative determination of adenovirus-mediated gene delivery to rat cardiac myocytes in vitro and in vivo. Proc Natl Acad Sci USA 1993;90(24):11498–11502.

[22] Sakamoto S, Tezuka K, Tsuji T, Hori NTamatani T. AILIM/ICOS: its expression and functional analysis with monoclonal antibodies. Hybrid Hybridomics 2001;20(5–6):293–303.

[23] Ono KLindsey ES. Improved technique of heart transplantation in rats. J Thorac Cardiovasc Surg 1969;57(2):225–229.

[24] Heron I. A technique for accessory cervical heart transplantation in rabbits and rats. Acta Pathol Microbiol Scand A 1971;79(4):366–372.

[25] Lin H, Bolling SF, Linsley PS, et al. Long-term acceptance of major histocompatibility complex mismatched cardiac allografts induced by CTLA4Ig plus donor-specific transfusion. J Exp Med 1993;178(5):1801–1806.

[26] Yin D, Fathman CG. Induction of tolerance to heart allografts in high responder rats by combining anti-CD4 with CTLA4Ig. J Immunol 1995;155(4):1655–1659.

[27] Jones ND, Turvey SE, Van Maurik A, et al. Differential susceptibility of heart, skin, and islet allografts to T cell-mediated rejection. J Immunol 2001;166(4):2824–2830.

[28] Sakaguchi S, Sakaguchi N, Asano M, Itoh M, Toda M. Immunologic self-tolerance maintained by activated T cells expressing IL-2 receptor alpha-chains (CD25). Breakdown of a single mechanism of self-tolerance causes various autoimmune diseases. J Immunol 1995;155(3):1151–1164.

[29] Shevach EM. Regulatory T cells in autoimmmunity. Annu Rev Immunol 2000;18:423–449.

[30] Takahashi T, Kuniyasu Y, Toda M, et al. Immunologic self-tolerance maintained by $CD25^{+}CD4^{+}$ naturally anergic and suppressive T cells: induction of autoimmune disease by breaking their anergic/suppressive state. Int Immunol 1998;10(12):1969–1980.

[31] Tamatani T, Tezuka K, Hanzawa-Higuchi N. AILIM/ICOS: a novel lymphocyte adhesion molecule. Int Immunol 2000;12(1):51–55.

Overexpression of Retinoic Acid Receptor α in Hepatocellular Carcinoma[1]

Keiji Sano,[2] Tadatoshi Takayama, Koji Murakami, Ikuo Saiki, and Masatoshi Makuuchi

Hepato-Biliary-Pancreatic Surgery Division, Artificial Organ and Transplantation Surgery Division, Department of Surgery, Graduate School of Medicine, University of Tokyo, Tokyo 113-8655, Japan [K. S., T. T., M. M.], and Department of Pathogenic Biochemistry, Research Institute for Wakan-Yaku, Toyama Medical and Pharmaceutical University, Toyama 931-0194, Japan [K. M., I. S.]

ABSTRACT

Purpose: **Retinoid analogues have been reported to inhibit the growth of hepatocellular carcinoma (HCC). However, the expression profile of retinoic acid receptors (RARs) in HCC has not been fully clarified. In this study, we investigated the expression of RAR mRNAs and proteins in resected HCC and nontumor liver tissue.**

Experimental Design: **Reverse transcription-PCR and Western blot analysis were applied to investigate the expression of RAR mRNAs and proteins in 32 resected samples of HCC and 14 samples of nontumor liver tissue. A HCC cell line and primary-cultured hepatocyte were treated with RAR-α-selective retinoids *in vitro* to estimate their antiproliferative activity.**

Results: **The intensities of mRNA and protein for RAR-α in HCC tissue were significantly higher than those in nontumor liver tissue ($P = 0.002$ and $P = 0.002$, respectively). The intensity ratios of HCC *versus* nontumor liver for RAR-α mRNA and protein were significantly higher than those for RAR-β and RAR-γ (mRNA, $P = 0.02$ and $P = 0.006$; protein, $P = 0.04$ and $P = 0.007$, respectively). There was only one significant correlation between the higher intensity of RAR-β protein and tumor stage (stage I/II *versus* stage III/IVA, $P = 0.01$) among clinicopathological variables in the HCC patients. However, *in vitro* experiments showed that the growth of a RAR-α-elevated HCC cell line was potently inhibited by treatment with retinoids at concentrations that did not affect the growth of primary-cultured hepatocytes.**

Conclusions: **These results imply that RAR-α is the dominant receptor in HCC, which suggests that RAR-α-selective retinoid analogues may be useful for chemotherapy.**

INTRODUCTION

HCC[3] is one of the most common malignancies worldwide and causes almost 1 million deaths annually (1, 2). Although early diagnosis and surgical treatment improve survival (3), long-term survival is still unsatisfactory because of a high incidence of recurrence, which may be reduced by some novel options (4, 5). The prognosis of unresectable cases remains poor (6) because effective antitumor drugs are not yet available (7).

Retinoids, vitamin A analogues, strongly affect embryogenesis, differentiation, and carcinogenesis (8). The biological activity of retinoids is exerted through binding to specific nuclear receptors in the steroid/thyroid hormone family. Two major classes of retinoid receptors, RARs and retinoic X receptors, have been identified, each of which consists of three distinct receptor subtypes: α; β; and γ (8). Clinically, the successful treatment of patients with acute promyelocytic leukemia with ATRA, a natural retinoid, is well documented (9). However, the failure of long-term treatment has been reported due to the enhancement of plasma clearance (10) and to the induction of several metabolizing enzymes in the liver that inactivate retinoic acid (11). Moreover, in a Phase II trial, oral treatment with ATRA was reported to be ineffective against unresectable HCC (12).

The relationship among receptor subtype expressions has been investigated, for instance, in lung cancer (13), and some receptor-selective retinoids that bind to and transactivate specific retinoid receptors have been shown to be effective against non-small cell lung cancer (14) and HCC (4). RXR-α has been described as highly expressed in human HCC and possibly responsible for the aberrant growth of HCC (15, 16). As for RARs, we reported previously that an *in vitro*-established HCC cell line showed an elevated expression of RAR-α, compared with RAR-β, and -γ, and responded to RAR-α-selective retinoids with regard to inhibition of cell proliferation (17). However, the expression profile of RARs in HCC tissue from resected specimens remains to be investigated.

In this study, we investigated the expression of RARs in

Received 10/16/02; revised 3/13/03; accepted 3/31/03.
The costs of publication of this article were defrayed in part by the payment of page charges. This article must therefore be hereby marked *advertisement* in accordance with 18 U.S.C. Section 1734 solely to indicate this fact.
[1] Supported in part by a grant-in-aid for cancer research from the Ministry of Health and Welfare, Tokyo, Japan.
[2] To whom requests for reprints should be addressed, at Hepato-Biliary-Pancreatic Surgery Division, Artificial Organ and Transplantation Surgery Division, Department of Surgery, Graduate School of Medicine, University of Tokyo, 7-3-1 Hongo, Bunkyo-ku, Tokyo 113-8655, Japan. Phone: 81-3-5800-8654; Fax: 81-3-5684-3989; E-mail: SANO-2SU@h.u-tokyo.ac.jp.

[3] The abbreviations used are: HCC, hepatocellular carcinoma; RAR, retinoic acid receptor; ATRA, all-*trans* retinoic acid; RT-PCR, reverse transcription-PCR; AP-1, activator protein 1; TAC-101, 4-[3,5-bis(trimethylsilyl)benzamido] benzoic acid; GAPDH, glyceraldehyde-3-phosphate dehydrogenase; T/N, tumor *versus* nontumor intensity; TNM, tumor-node-metastasis.

HCC to evaluate the potential for the clinical application of retinoic acid derivatives to treat HCC.

MATERIALS AND METHODS

Patients. Between September 1999 and February 2000, we performed hepatectomy in 32 consecutive patients with HCC. Fresh surgical specimens of HCC and paired nontumor liver tissue (5 mm in cube), more than 1 cm away from the HCC, were obtained.

Cell Lines and Chemicals. The HCC cell line JHH-7 was kindly provided by Dr. S. Nagamori (Jikei University School of Medicine, Tokyo, Japan), and primary-cultured hepatocytes were purchased from Cell Systems Co. (Kirkland, WA). Both cells were maintained as monolayer cultures in CS-C medium (Cell Systems Co.) at 37°C in a humidified atmosphere of 5% CO_2/95% air. TAC-101, which shows selective binding affinity for RAR-α, was provided by TAIHO Pharmaceutical Co. Ltd. (Tokyo, Japan). ATRA was purchased from WAKO Pure Chemical Industries Ltd. (Tokyo, Japan). Both reagents were dissolved in DMSO at a concentration of 20 mM before use. Antibody for RARs was purchased from Santa Cruz Biotechnology (Santa Cruz, CA). Horseradish peroxidase-conjugated goat antirabbit antibody was purchased from Amersham (Piscataway, NJ).

RT-PCR. RT-PCR was used to detect mRNA for RARs and GAPDH (17). Total RNA from HCC and nontumor tissue was extracted using Isogen (Nippon Gene Inc., Toyama, Japan) in 14 patients. In the other 18 patients, only HCC tissues were analyzed for a more precise analysis. First-strand cDNA was prepared from RNA using 1 unit of avian myeloblastosis virus reverse transcriptase, 5 μg of total RNA as a template, and 10 ng/ml poly$(dT)_{12-18}$ oligonucleotide in the presence of 10 mM DTT and 0.5 unit of RNase inhibitor (Life Science Inc.). The reverse transcription reaction profile was 95°C for 3 min, 4°C for 10 min, and 42°C for 45 min. PCR amplification consisted of denaturation at 94°C for 30 s, annealing at 56°C (RAR-β and GAPDH) or 60°C (RAR-α and RAR-γ), and extension at 72°C for 1 min and 30 s, using template cDNA and a TAKARA Ex Taq PCR kit (Takara Shuzo Co., Ltd., Kyoto, Japan). The PCR products for RAR-α, RAR-β, RAR-γ, and GAPDH were amplified at 33, 36, 36, and 27 cycles, respectively. Each cycle was determined from preliminary experiments with various amplification cycles in each of the RARs extracted from the HCC cell line JHH-7 and hepatocytes. Each assay was performed in triplicate. The sequences of primers have been described previously (18). The PCR products were electrophoresed on 1.5% agarose gel and detected by ethidium bromide staining. The relative abundance of mRNA for RARs was expressed as intensity ratios relative to GAPDH, as determined at appropriate amplification cycles (exponential phase) using the Master Scan Gel Analysis System (Scanalytics, Billerica, MA).

Western Blot Analysis. Nucleoprotein of HCC and nontumor specimens (5 mm in diameter) was extracted using a nuclear and cytoplasmic extraction reagents kit (Pierce, Rockford, IL). Extracted protein (5 μg) was electrophoresed on polyacrylamide gel (19). The gels were blotted onto nitrocellulose filters (Bio-Rad, Hercules, CA). The filters were developed with rabbit polyclonal antibodies specific for RAR-α, RAR-β, and RAR-γ (4°C, overnight), horseradish peroxidase-conjugated goat antirabbit antibody (room temperature, 2 h), and SuperSignal (Pierce) detection.

Table 1 Expression levels of mRNA for RARs

Total RNA of HCC tissues and matched liver tissues was reverse-transcribed, and the cDNA products were used for PCR. To compare the expression levels of mRNAs for RARs semiquantitatively, the intensity ratios relative to those for GAPDH were determined at appropriate amplification cycles (exponential phase) using the Master Scan Gel Analysis System. Data are given as mean ± SD.

	Intensity (RARs/GAPDH)		
	Nontumor tissue (n = 14)	HCC tissue (n = 31)	P^a
RAR-α	0.534 ± 0.442	1.021 ± 0.373	0.002
RAR-β	0.943 ± 0.458	0.845 ± 0.340	0.482
RAR-γ	0.824 ± 0.397	0.712 ± 0.483	0.418

[a] Two-tailed Welch's t test was performed.

Semiquantitative Analysis. The intensity of mRNA for RARs in RT-PCR analysis was semiquantified using a density ratio to GAPDH at appropriate amplification cycles (exponential phase), determined with the Master Scan Gel Analysis System (Scanalytics). The intensity of each RAR protein was also semiquantitatively determined by analyzing electrophoresis product in Western blot analysis from each 5 μg of extracted nuclear protein.

Clinical Correlation of RARs. The intensities of mRNA for RARs and protein of RARs in 32 HCC tissues were compared with regard to several clinical factors: age; sex (male *versus* female); tumor size; α-fetoprotein; des-γ-carboxyprothrombin; hepatic virus infection (hepatic B virus infection *versus* hepatic C virus); stage grouping [stage I or II *versus* stage III or IVA (20)], histological differentiation (well differentiated *versus* moderate or poorly differentiated), vascular invasion (positive *versus* negative), and background liver (normal liver or chronic hepatitis *versus* liver cirrhosis).

Assay for *in Vitro* Antiproliferative Activity. JHH-7 cells and hepatocytes were seeded (4000 cells/well) into 96-well culture plates. After 24 h of incubation, various concentrations of TAC-101 or ATRA were added to the culture plates. After 72 h of incubation, crystal violet staining was performed as described previously with some modification (18).

Statistical Analysis. The significance of differences in the intensity, intensity ratio, and clinicopathological variables (sex, hepatic virus infection, stage grouping, histological differentiation, vascular invasion, and background liver) was assessed using the two-tailed Welch's t test. Other clinicopathological variables (age, tumor size, α-fetoprotein, and PIVKA-II) were examined by Spearman's rank correlation coefficient test. Differences at $P < 0.05$ were considered to be statistically significant.

RESULTS

Intensity of mRNA for RARs. Intensity for RAR-α in tumor tissue was significantly higher than that in liver tissue (1.021 ± 0.373 *versus* 0.534 ± 0.442; $P = 0.002$). There was no significant difference in the intensities for RAR-β and RAR-γ between the tumor and liver (Table 1).

Table 2 Expression levels of protein for RARs

Nuclear protein was extracted from HCC tissues and matched liver tissues. Western blot analysis was performed using extracted protein (0.005 mg/lane). The intensity of each proteins was determined using the Master Scan Gel Analysis System. Data are given as mean ± SD.

	Intensity (RARs/5 μg protein)		
	Nontumor tissue (n = 14)	HCC tissue (n = 31)	P^a
RAR-α	1228.3 ± 645.0	2027.5 ± 973.7	0.002
RAR-β	918.2 ± 435.6	936.1 ± 742.3	0.920
RAR-γ	412.6 ± 193.1	372.1 ± 123.0	0.559

[a] Two-tailed Welch's t test was performed.

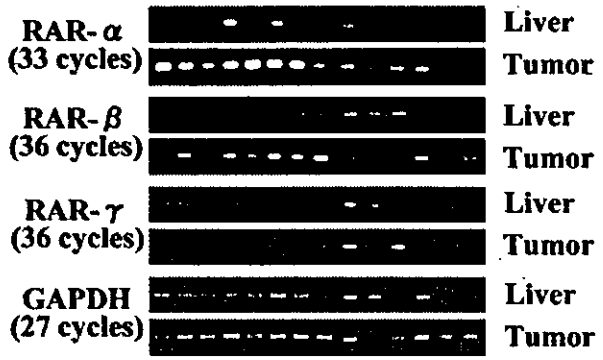

Fig. 1 Expression of mRNA for RARs in the nuclear fraction of HCC tissues and matched liver tissues. The PCR products for RAR-α, RAR-β, RAR-γ, and GAPDH were amplified at 33, 36, 36, and 27 cycles, respectively, and electrophoresed on 1.5% agarose gels. The products were visualized by ethidium bromide staining.

Detection of RAR-α, RAR-β, and RAR-γ Protein by Western Blot. There was a significant difference in the intensity of RAR-α between HCC and liver tissue (2027.5 ± 973.7 *versus* 1228.3 ± 645.0, P = 0.002), but not in RAR-β or RAR-γ (Table 2).

Tumor *versus* Nontumor Intensity Ratio. To assess the intensity ratio in individual patients, we calculated a T/N ratio of mRNA for RARs (Fig. 1) and RAR proteins (Fig. 2) in 14 patients. The T/N ratio of mRNA for RAR-α was significantly higher than those for RAR-β and RAR-γ (P = 0.02 for RAR-β and P = 0.006 for RAR-γ). The T/N ratio of RAR-α protein was also higher than those of the other two RARs (P = 0.04 for RAR-β and P = 0.007 for RAR-γ; Table 3).

Clinical Correlation of RARs. The correlations between expression levels of RAR-α, RAR-β, and RAR-γ and several clinical factors were analyzed. Only one significant difference was found in the intensity of RAR-β protein between the intensity in TNM stage I or II HCC and that in TNM stage III or IVA HCC (P = 0.01).

***In Vitro* Antiproliferative Activity of Retinoids.** We used RAR-α-selective retinoid (TAC-101) and RAR pan-agonist (ATRA) to test *in vitro* antiproliferative activity. As shown in Fig. 3*A*, both TAC-101 and ATRA potently inhibited the proliferation of the HCC cell line JHH-7, which shows high levels of RAR-α expression. TAC-101 was more effective than ATRA at inhibiting the proliferation of this HCC cell line. No severe antiproliferative effects were seen in hepatocytes treated with TAC-101 or ATRA (Fig. 3*B*). IC_{50} values of TAC-101 and ATRA were 0.96 and 2.89 μM for JHH-7, respectively, whereas these were each >10 μM for hepatocytes.

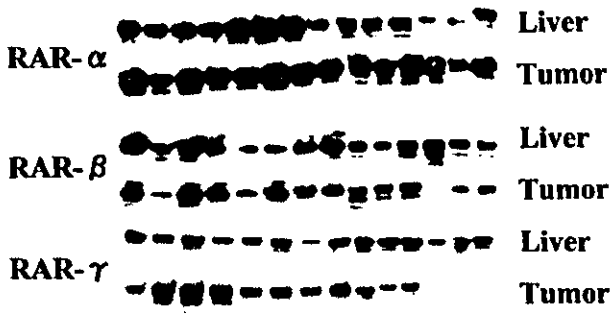

Fig. 2 Expression of RAR proteins in the nuclear fraction of HCC tissues and matched liver tissues. Extracted protein (5 μg/lane) was electrophoresed on polyacrylamide gel. The gels were blotted onto nitrocellulose filters (Bio-Rad). The filters were developed with rabbit polyclonal antibodies specific for the RAR-α, RAR-β, RAR-γ, and horseradish peroxidase-conjugated goat antirabbit antibody and detected by SuperSignal solution.

Table 3 T/N ratios of mRNA for RARs and RAR proteins

Nuclear protein was extracted from HCC tissues and matched liver tissues. Western blot analysis was performed using extracted protein (0.005 mg/lane). The intensity of each proteins was determined using the Master Scan Gel Analysis System. Data are given as mean ± SD.

	T/N ratios	
	mRNA	Protein
RAR-α	3.35 ± 2.59[a,b]	3.12 ± 2.58[c,d]
RAR-β	1.27 ± 0.88[a]	1.46 ± 0.95[c]
RAR-γ	1.06 ± 0.36[b]	0.91 ± 0.47[d]

[a] P = 0.02.
[b] P = 0.006.
[c] P = 0.04.
[d] P = 0.007.

DISCUSSION

We found significantly higher expression levels of RAR-α (both mRNA and protein levels) in HCC tissue than in nontumor tissue, whereas there were no differences in the expression levels of RAR-β and RAR-γ between tumor and nontumor tissues. We first confirmed the preferential expression of RAR-α in resected tissues, as shown previously in cell lines (17, 18, 21).

Ligand-binding RARs form heterodimeric units with retinoid X receptors (22) and induce various biological effects including differentiation (23), apoptosis (24), and antimetastatic (25) and antiangiogenic activity (26). A tight link exists between the expression of specific retinoid receptors and preclinical or clinical retinoid responses. Some retinoids have been reported to induce apoptosis in human lung cancer cells via RAR-α (27). We showed previously that TAC-101, a novel benzoic acid derivative that shows selective binding affinity for RAR-α, induces apoptosis not only in a HCC cell line *in vitro* but also in

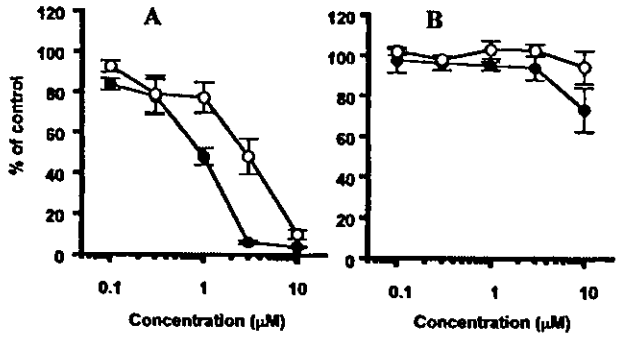

Fig. 3 Antiproliferative activity of retinoids against HCC and primary-cultured hepatocyte. JHH-7, a hepatocellular carcinoma cell line (*A*), and primary-cultured hepatocyte (*B*) were treated with TAC-101 (●) or ATRA (○) for 72 h. The antiproliferative activity was determined by crystal violet colorimetric assay.

a tumor tissue section of TAC-101-treated mice *in vivo* (18). Therefore, RAR-α-selective retinoids may induce apoptosis in HCC via RAR-α-mediated signals to give an antitumor effect.

TAC-101 also shows AP-1 antagonism, perhaps via RAR-α (28, 29). Increased AP-1 activity is associated with carcinogenesis in some malignancies (30). Antagonism of AP-1 by retinoic acid has been reported to inhibit malignant transformation. In addition, RAR-α-dependent antagonism of AP-1 inhibited the growth of a lung cancer cell line (31). AP-1 is a heterodimeric transcription factor and consists of the oncoprotein Jun and Fos families. Although hepatocarcinogenesis is considered to be caused by multistep processes (32), in an analysis of 290 HCC patients, Yuen *et al.* (33) revealed that there was a positive association between the expression of c-Fos and the expression of c-Jun in HCC tissues. Thus, a RAR-α-selective retinoid, such as TAC-101, which shows potent AP-1 antagonism, may be beneficial not only for the therapeutic treatment of HCC but also for preventing secondary hepatocarcinogenesis.

HCC cells become well-differentiated to moderately or poorly differentiated as the tumor progresses (34, 35). In the human bronchus, the response to receptor-selective retinoids has been reported to vary among normal, premalignant, and malignant cells (36). In this study, the overexpression of RAR-α in tumor tissues of HCC was not significantly correlated with various clinical factors including tumor cell differentiation, tumor size, tumor markers, or tumor staging. On the other hand, the intensity of RAR-β protein was significantly higher in early-stage HCC compared with advanced-stage HCC. RAR-β was also reported to play important roles in differentiation and antiproliferation in hepatoma cells (37). Therefore, to clarify the possible preventive effect on malignant transformation in hepatocarcinogenesis, additional studies are needed, because no premalignant tumors were examined in this study.

We have already demonstrated that an *in vitro*-established HCC cell line responded to RAR-α-selective retinoids with regard to the inhibition of cell proliferation (17). Following that result, *in vitro* experiments in this study showed that the growth of a RAR-α-elevated HCC cell line was potently inhibited by treatment with retinoids at concentrations that did not affect the growth of primary-cultured hepatocytes. Moreover, at the same concentration, TAC-101 was more effective than panagonist, ATRA at inhibiting the proliferation of the HCC cell line. Retinoid resistance may be due to decreasing plasma levels resulting from a consistent acceleration of ATRA metabolism (10). Therefore, TAC-101 can be expected to be effective without resistance for longer periods than ATRA. It may be possible to avoid the adverse effects associated with chronic administration of high doses of retinoids because the dosage of TAC-101 can be smaller than that of ATRA. However, this cannot be predicted with great certainty because synthetic retinoids, which may not have the same biological properties as vitamin A, may also have different adverse effects (38).

In conclusion, the present study revealed that RAR-α was a dominant receptor for HCC in resected specimens, suggesting that RAR-α-selective retinoic acid derivatives may be clinically useful for chemotherapy in HCC patients.

ACKNOWLEDGMENTS

We thank Yuji Yamada, Dr. Toshiyuki Toko, Kenji Kitazato (Taiho Pharmaceutical Co., Ltd., Hanno Research Center), and Dr. Seishi Nagamori (Jikei University School of Medicine) for helpful comments and guidance in this study.

REFERENCES

1. El-Serag, H. B., and Mason, A. C. Rising incidence of hepatocellular carcinoma in the United States. N. Engl. J. Med., *340:* 745–750, 1999.

2. Taylor-Robinson, S. D., Foster, G. R., Arora, S., Hargreaves, S., and Thomas, H. C. Increase in primary liver cancer in the UK, 1979–94. Lancet, *350:* 1142–1143, 1997.

3. Takayama, T., Makuuchi, M., Hirohashi, S., Sakamoto, M., Yamamoto, J., Shimada, K., Kosuge, T., Okada, S., Takayasu, K., and Yamasaki, S. Early hepatocellular carcinoma as an entity with a high rate of surgical cure. Hepatology, *28:* 1241–1246, 1998.

4. Muto, Y., Moriwaki, H., Ninomiya, M., Adachi, S., Saito, A., Takasaki, K. T., Tanaka, T., Tsurumi, K., Okuno, M., Tomita, E., Nakamura, T., and Kojima, T. Prevention of second primary tumors by an acyclic retinoid, polyprenoic acid, in patients with hepatocellular carcinoma. N. Engl. J. Med., *340:* 1046–1047, 1999.

5. Takayama, T., Sekine, T., Makuuchi, M., Yamasaki, S., Kosuge, T., Yamamoto, J., Shimada, K., Sakamoto, M., Hirohashi, S., Ohashi, Y., and Kakizoe, T. Adoptive immunotherapy to lower postsurgical recurrence rates of hepatocellular carcinoma: a randomised trial. Lancet, *356:* 802–807, 2000.

6. Villa, E., Moles, A., Ferretti, I., Buttafoco, P., Grottola, A., Del Buono, M., De Santis, M., and Manenti, F. Natural history of inoperable hepatocellular carcinoma: estrogen receptor's status in the tumor is the strongest prognostic factor for survival. Hepatology, *32:* 233–238, 2000.

7. Venook, A. P. Treatment of hepatocellular carcinoma: too many options? J. Clin. Oncol., *12:* 1323–1334, 1994.

8. De Luca, L. M. Retinoids and their receptors in differentiation, embryogenesis, and neoplasia. FASEB J., *5:* 2924–2933, 1991.

9. Wang, Z. Y., Sun, G. L., Lu, J. X., Gu, L. J., Huang, M. E., and Chen, S. R. Treatment of acute promyelocytic leukemia with all-*trans* retinoic acid in China. Nouv. Rev. Fr. Hematol., *32:* 34–36, 1990.

10. Muindi, J., Frankel, S. R., Miller, W. H., Jr., Jakubowski, A., Scheinberg, D. A., Young, C. W., Dmitrovsky, E., and Warrell, R. P., Jr. Continuous treatment with all-*trans* retinoic acid causes a progressive reduction in plasma drug concentrations: implications for relapse and retinoid "resistance" in patients with acute promyelocytic leukemia. Blood, *79:* 299–303, 1992.

11. Adedoyin, A., Stiff, D. D., Smith, D. C., Romkes, M., Bahnson, R. C., Day, R., Hofacker, J., Branch, R. A., and Trump, D. L. All-*trans*